UPPSALA UNIVERSITET

FYSMAS1050

Examensarbete 30 hp
November 2016

# The ultraviolet spectral slope of high-redshift galaxies

Ludvig Sjöbom

Masterprogrammet i fysik
*Master Programme in Physics*

UPPSALA
UNIVERSITET

**Teknisk- naturvetenskaplig fakultet**
**UTH-enheten**

Besöksadress:
Ångströmlaboratoriet
Lägerhyddsvägen 1
Hus 4, Plan 0

Postadress:
Box 536
751 21 Uppsala

Telefon:
018 – 471 30 03

Telefax:
018 – 471 30 00

Hemsida:
http://www.teknat.uu.se/student

# Abstract

## The ultraviolet spectral slope of high-redshift galaxies

*Ludvig Sjöbom*

The slope of the ultraviolet continuum emissions from a galaxy between 1250 and 2600 Å provides insights about several facets of the galaxy. Mainly, it is well-correlated with the amount of dust. This work presents a search for objects whose UV-continuum slopes are excessively steep, as well as suggestions for follow-up. The method used is looking through existing data sets, and proposing follow-up of the outliers in the distribution of slopes. Close to fifteen objects with slopes beyond what is easily explained by theory are presented. Since these lie beyond the realm of current theories, confirmations of these may hint at more extreme stellar populations than those currently known. This may include excessively metal-poor stars such as population III stars, or stellar populations where the initial mass function (IMF) for some reason may be biased towards massive stars. Steeper slopes are in general indicative of a lack of dust and an abundance of hot, blue stars; this is due to the reddening caused by dust, and emissions from cooler stars being peaked at longer wavelengths.

Handledare: Erik Zackrisson
Ämnesgranskare: Kjell Olofsson
Examinator: Andreas Korn
FYSMAS1050

# Popular science summary in Swedish

## Populärvetenskaplig sammanfattning på svenska

En galax är inte bara en vit fläck på himlen. En noggrannare studie ger att ljuset är fördelat mellan de olika färgerna, så att vi ser mer rött än grönt, eller mer blått. Självklart sträcker sig denna fördelning av färger utanför det vi kan se, förbi ultraviolett och infrarött till röntgenstrålning och radiovågor. Eftersom galaxer till stor del är samlingar av stjärnor, säger fördelningen av ljuset oss något om vilka stjärnor som ingår i galaxen. Till det här arbete är det främst det ultravioletta ljuset som är intressant, eftersom det säger oss mycket om åldern på stjärnorna, samt stoftinnehållet i galaxen.

Våglängdsfördelningen hos den ultravioletta delen av ljuset kan parametriseras med $\beta$, beta. $\beta$ säger då, i grova drag, något om lutningen på distributionen av ljus när man ritar upp en graf på våglängd mot intensitet. Detta är praktiskt, eftersom man kokar ner informationen till ett tal, som kan jämföras med $\beta$ för andra galaxer. Den här lutningen beror alltså på hur ljuset är fördelat mellan långa och korta våglängder, mer kortvågigt ljus ger en brantare kurva, på samma sätt ger långvågigt ljus en flackare. Beroende på värde kan $\beta$ kallas *blåare* eller *rödare*. Det kan tyckas ointuitivt, men syftar på om distributionen av ljus är förskjuten åt kortare eller längre våglängder, där blåare är brantare och rödare är flackare. I analogi med synligt ljus där blått ljus har kortare våglängd än rött, kallas $\beta$ för blåare om det är en övervikt mot kortare våglängder, och rödare om det är mer långvågigt ljus. Det ska dock kommas ihåg att de längre våglängderna fortfarande är klart utanför det synliga området.

Vad är det då som avgör färgen på en galax? Till att börja med kan vi tänka oss en galax fylld enbart med stjärnor, ljuset kommer således från dessa, och ingenting annat. Färgen hos en stjärna avgörs av dess massa, där tyngre stjärnor sänder ut det mesta av sitt ljus i ultraviolett och lättare stjärnor åt det infraröda hållet. Dessutom bestämmer en stjärnas massa dess livslängd, på det viset att en tyngre stjärna utvecklas och dör fortare, lättare stjärnor lever på motsvarande sätt längre. Sammantaget gör detta att en mycket blå galax måste innehålla en mycket stor andel tunga stjärnor, och dessutom inte vara allt för gammal.

Åt andra hållet kan vi fundera på vad som gör en galax rödare. Till att börja med kan det vara så enkelt som att det saknas blå stjärnor. Detta kan tyda på en äldre galax, där de blå stjärnorna dött ut. En annan förklaring kräver att vi justerar modellen av en galax som endast innehåller stjärnor. Om vi lägger till stoft i galaxen kommer vi med stor sannolikhet få en rödare galax, eftersom det ultravioletta ljuset fastnar i och värmer upp stoftet. Det varma stoftet strålar sedan ut energin som värmestrålning, infrarött ljus. Med tunga, varma stjärnor kommer en betydande andel av ljuset vara tillräckligt energirikt för att jonisera det väte som kan finnas i en galax. Detta leder också till en förskjutning åt det röda hållet eftersom det ultravioletta går åt till joniseringen, och joniserat väte lyser starkt i en vacker, röd färg.

Syftet med det här arbetet har varit att leta igenom tidigare studier som hat mätt $\beta$ för ett stort antal galaxer, och sedan se om det finns tecken på galaxer som inte passar in i vår förståelse av $\beta$. I det här fallet har fokus varit riktat åt de blåare värden som uppmätts, eftersom det kan tyda på att det finns något nytt att lära sig om unga galaxer och dess mängd tunga grundämnen. För att få lite mer klarhet i bakgrunden till oväntat blå värden innehåller det här arbetet även förslag på uppföljning med bättre instrument. Resultatet av arbetet är en lista med koordinater och värden på $\beta$ för omkring ett dussin galaxer. Dessa är intressanta eftersom de inte passar in i dagens kunskap om vilka värden på $\beta$ som är möjliga.

# Contents

# List of Figures

# List of Tables

# 1. Introduction

Galaxies commonly emit electromagnetic radiation over a wide range of wavelengths. The ultraviolet part of the emitted light contains information on various facets of the state of the galaxy. The UV continuum between roughly 1250 Å and 2600 Å is commonly parametrized as a power law of the form $f_\lambda \propto \lambda^\beta$. This parametrization was first introduced by Calzetti et al. (1994) as a means of studying the effects of dust extinction in galaxies, and has later been shown to trace the dust extinction at higher redshifts, as well as being correlated with far-infrared dust emission (see e.g. Finkelstein et al. 2012, Meurer et al. 1999, Reddy et al. 2012).

Following Calzetti et al. (1994), one finds $\beta$ by performing a linear fit in the $\log f - \log \lambda$ plane of the observed spectrum. The original definition includes a few 'windows' in $\lambda$, intended to make $\beta$ less sensitive to various features in the spectrum and better reflect the *continuum.* These windows are implemented by removing the data points at certain intervals in $\lambda$, and doing the linear fit to the remaining data points. The upper and lower limits of $\lambda$ used in determining $\beta$ are 1268 and 2580 Å, respectively. Hence, $\beta$ probes the ultraviolet spectrum redward of the Ly$\alpha$ line.

Common values of $\beta$ are around -2 (e.g. Bouwens et al. 2014). More positive values are known as *redder*, while more negative values are *bluer*. According to Finkelstein et al. (2012), the values of $\beta$ for various galaxies usually range from -2.5 to -0.5, with -2.7 being close to the limit of what can be explained by a population of young, unreddened stars of low metallicity.

## 1.1. Underlying physics of $\beta$

Galaxies are essentially collections of stars. Therefore, the light emitted by a galaxy in the optical and near-infrared is for the most part due to starlight (e.g. Schneider 2015). Of course, this is not the only source of light in a galaxy. The model of the way Active Galactic Nuclei (AGN) produce their light is via infall of material on the accretion disc of a massive black hole, and having accreted material accelerated by the enormous gravitational potential. An AGN may also have relativistic jets of plasma ejected along the axis of rotation, possibly feeding radio lobes of gas far from the central black hole.

The accretion disc is then the main source of optical and UV continuum emission. Thus, a galaxy with an AGN may get a far bluer UV continuum than a similar galaxy, lacking the AGN. Hence, care needs to be taken to exclude the possibility of an AGN when a galaxy is found with an excessively blue $\beta$, before one jumps to conclusions about its origins.

When one deals with bright, hot stars, the possibility of producing photons of sufficient energy to ionize hydrogen becomes rather large. Indeed, this is often observed in the form of emission nebulae, in which clouds of hydrogen are ionized by UV photons and subsequently recombine. This causes an overall loss of UV photons, and one instead gets a H II region. H II regions emit strongly in the Balmer series, and are thus usually red from the H$\alpha$ line at 6563 Å.

Consider a galaxy containing nothing but stars, we thus see the sum of the starlight. Since $\beta$ is a probe of the overall light from the galaxy, it will be sensitive to features of the light from the stellar population. The wavelength region probed by $\beta$ is in the rest-frame ultraviolet. This means that the slope of the UV continuum is strongly affected by the amount of bright, hot stars, such as O or B giants.

O and B stars are very massive, and thus these types of stars evolve quickly, meaning that a young galaxy will have more of them than an old galaxy. This will then lead to a bluer value for $\beta$. The quick evolution also means that a redder galaxy may have its UV slope boosted by a period of star formation, since this will replenish the population of hot, bright stars. This means that the value of $\beta$ is dependent on the star formation history.

The shape of the UV continuum of a galaxy stays fairly constant over a relatively large range of ages. The reason for this is that the peak of the Planck function for such a massive star is far blueward of the region of interest here; $\beta$ thus probes the Rayleigh-Jeans part of the stars' spectrum, which is not very age-sensitive.

The overall metallicity of a galaxy also plays a role in setting the value of $\beta$, since stars formed by gas of low metallicity will be bluer.

The value of $\beta$ is also sensitive to the initial mass function (IMF), since this describes the amount of stars formed in a given mass bracket. A top-heavy IMF will provide a bluer values of $\beta$, since a higher fraction of the gas will form massive stars.

Of course, the star of the show is dust. Indeed, this was part of the motivation for defining $\beta$ in the first place. In broad strokes, the mechanism by which dust affects the spectral shape of a galaxy is by absorbing UV photons, and subsequently re-emitting them as IR photons. This is accomplished simply by the dust being heated by the UV light, with the re-emission being driven by thermal radiation from the now slightly warmer grains of dust. Naturally, since the dust does not absorb all starlight, and has a far larger surface area than the stars, the temperature will be a lot cooler than that of the typical O or B star. $\beta$ has been shown to be well-correlated with the amount of dust, in that dustier galaxies generally have redder $\beta$s. This is rather reasonable, since more dust increases the optical depth, and thus increases the likelihood of photon-dust interactions.

The picture is made more complicated by the possibility of various geometrical configurations of the dust, which may scatter sidebound UV photons into the line of sight, thus increasing the observed UV flux.

## 1.2. Determining $\beta$

There are three main methods of determining $\beta$, each with its own advantages and drawbacks.

One method is the one stated above, performing a least-squares fit to the $\log f - \log \lambda$ plane of an observed spectrum as done by e.g. Calzetti et al. (1994). Since one is not interested in spectral lines in this context, one needs not have a high-resolution spectrum. This means that the measurement of $\beta$ can be done as a quick check using low-resolution spectrographs, and follow-up can be done with higher-resolution instruments; the trade-off being the usual: resolution versus signal in each wavelength bin. This method does — however — have a few drawbacks; most notably that the galaxy needs to be bright enough for spectroscopy, which thus excludes the faintest galaxies.

If spectroscopy of a galaxy is not available, all is yet not lost. Photometry may be used to estimate $\beta$ in a few ways. One can perform a power-law fit directly to the available bands, and thus get a value of $\beta$. This method was used by e.g. Bouwens et al. (2014) for galaxies where several bands were available. For the z $\approx$ 7 galaxies where only two bands of photometry were available, Bouwens et al. (2014) claimed that the power-law fit was equivalent to the fitting formula (their eq. 1)

$$\beta = -2.0 + 4.39(J_{125} - H_{160}).$$

A similar formula can be seen elsewhere in the literature, with the factor 4.39 often being different between authors. A direct fit to photometry can thus allow for measurements of $\beta$ for galaxies faint enough to be at the edge of detectability, at the cost of precision.

Another method of finding a value for $\beta$ is by performing spectral energy distribution (SED) fitting, as done by e.g Finkelstein et al. (2012) and Finkelstein et al. (2010). The method is based on synthetic stellar populations, of which a large grid of varying parameters is computed. The parameters being varied include age, metallicity, dust attenuation and star formation history. The advantages of this method are that more photometric bands may be used to put a constraint on $\beta$.

According to Rogers et al. (2013) and Bouwens et al. (2014), the SED fitting method may cause erroneous values if underlying assumptions on spectral shape, precise redshift or Ly$\alpha$ equivalent width are not met. If the galaxy has a higher Ly$\alpha$ equivalent width than assumed, the flux in the bluest band may be boosted, and a too steep slope will be inferred. The effect of Ly$\alpha$ may be rather significant at higher redshifts, since the observed equivalent width increases as $(1 + z)$, while the effective width of the filter decreases as $(1+z)^{-1}$(Finkelstein et al. 2010). Likewise, a too low estimate of the redshift will boost the bluer filter, leading to the same effect. Further, since this method is based on synthetic spectra, it is obviously not able to fully recover observations of objects falling outside the modelled region of the parameter space. In combination with the aforementioned sensitivity to systematic effects, this means that this method may not be appropriate for studies which are interested in populations of objects at the edge of parameter distribution.

## 1.3. Recent surveys

The previously mentioned photometric methods of determining $\beta$ have one great advantage: they are relatively cheap. This, of course, stems from the fact that photometry requires less available light from the galaxy for meaningful observations than does spectroscopy; two bands of photometry allows for a (somewhat crude) estimate of $\beta$, as opposed to spectroscopy, which requires enough light for a decent signal-to-noise ratio over lots of small wavelength bins—a problem that only becomes greater with increasing resolution.

Owing to this, large-scale photometric surveys have been carried out: allowing for statistically sound conclusions about the distribution of $\beta$ to be drawn.

In 2010, some controversy was sparked by claims of detections of galaxies having $\beta \sim -3$ (Bouwens et al. 2010b, Bouwens et al. 2010a). This was done using WFC3/IR Hubble data, and performing a two-filter power-law fit. However, these claims were later retracted, and Bouwens et al. (2014) claims that the measurements may be due to systematic colour bias. See e.g. fig. 10 in Bouwens et al. (2014), where the authors illustrate the effects of a small error in the colour measurement propagate into a rather large error in $\beta$.

Finkelstein et al. (2012) performed an analysis of the evolution of $\beta$ with redshift over the range $4 < z < 8$ in the data from the CANDELS Multi-cycle HST program as well as the HUDF and ERS programs. This was done using the above mentioned SED fitting method, in which model spectra were fit to the available photometry. The study found that there was significant evolution with redshift of the median $\beta$ for galaxies of varying luminosities over the redshift range sampled. The values of mean $\beta$ found were claimed to be consistent with little to no dust at z $\approx$ 7, and lower redshifts having dustier galaxies. The authors argue that this is consistent with the z = 7 galaxies producing their first generation of stars at z $\approx 15 - 20$, and that the onset of dust at z $< 7$ matches $M < 3.5 M_{\odot}$ stars evolving into the AGB phase and producing dust efficiently.

More recently, Bouwens et al. (2014) published an article in which over 4000 galaxies were investigated with the photometric power-law fit method. The galaxies under investigation were found in the HST HUDF/XDF, HUDF09-1, HUDF09-2, ERS, CANDELS-N and CANDELS-S data sets. The intention was to reconcile the inconsistencies between previous studies by performing a review of systematic errors, and measuring $\beta$ via a method robust against noise-driven biases. The authors emphasize that—particularly at higher redshift—the measured value of $\beta$ can be extraordinarily sensitive to small errors in the photometry, as well as the assumptions going into the modelling of galaxies. They found that the discrepancies between mean values of $\beta$ found in different studies can be reconciled by accounting for the systematic errors in each earlier study. Dividing the galaxies into redshift bins at z=[4, 5, 6, 7], the mean values of beta fall from $-2.03 \pm 0.03 \pm 0.06$ to $-2.30 \pm 0.18 \pm 0.13$. This is claimed to be consistent with a slight evolution of $\beta$ with cosmic time, if similar galaxies are sampled at all epochs. For galaxies of a given luminosity, $\beta$ is found to become bluer with increasing redshift. A correlation between $\beta$ and UV luminosity at z $\sim 7$ is also found.

## 1.4. This work

This work is intended to look through existing data sets of galaxies at redshifts above $\sim 1$. In these data sets, the distribution of $\beta$ for the galaxies will be searched for excessively blue outliers. Galaxies beyond the "normal" values will then be further investigated in terms of measurement uncertainties. A literature search will then be performed for those galaxies whose values of $\beta$ still lie beyond what is easily explained. Finally, a suggestion for follow-up of the remaining galaxies will be proposed.

# 2. Selection

## 2.1. Overall selection method

In order to keep the selection of galaxies homogeneous over different data sets a small MATLAB function was written. The function takes a data set, and selects galaxies where the stated $\beta$ plus its uncertainty are more negative than -2.7, to match the claims of Finkelstein et al. (2012) that values of $\beta$ around -2.7 are consistent with a low-metallicity population of young stars. To avoid excessively erroneous measurements, the function selects only those galaxies where the stated error in $\beta$ is lower than one. The uncertainty in $\beta$ can in some cases be found directly in the published data set, in other cases it must be estimated. An example of the former can be found in table 2.4, the data set of Dunlop et al. (2013). For an example of the latter, see section 2.2.2. In this work, the uncertainty in $\beta$ will be designated by $\sigma_\beta$.

The output of the function is a list of the galaxies deemed interesting, indices for retrieving those galaxies from the data set and a plot of the $\beta - \sigma_\beta$ plane, in which the limits for selection and selected galaxies are highlighted. An example of the output is shown in fig. 2.1.

Due to its nature as a function, the galaxy-selecting code can easily accommodate various data sets, as long as an ID along with an estimate of $\beta$ and its associated uncertainty are given.

The code for the function can be found in appendix A.1.

## 2.2. VUDS galaxies

A sample of spectroscopic galaxies can be found in the Vimos Ultra-Deep Survey (VUDS), which is intended to cover redshifts in the interval $2 < z \simeq 6$ (Le Fèvre et al. 2015). The VUDS data is to be made public in several data releases, each of which will contain part of the total data set. The first data release is aptly named VUDS DR1 (Tasca et al. 2016), and contains spectra of close to 700 galaxies.

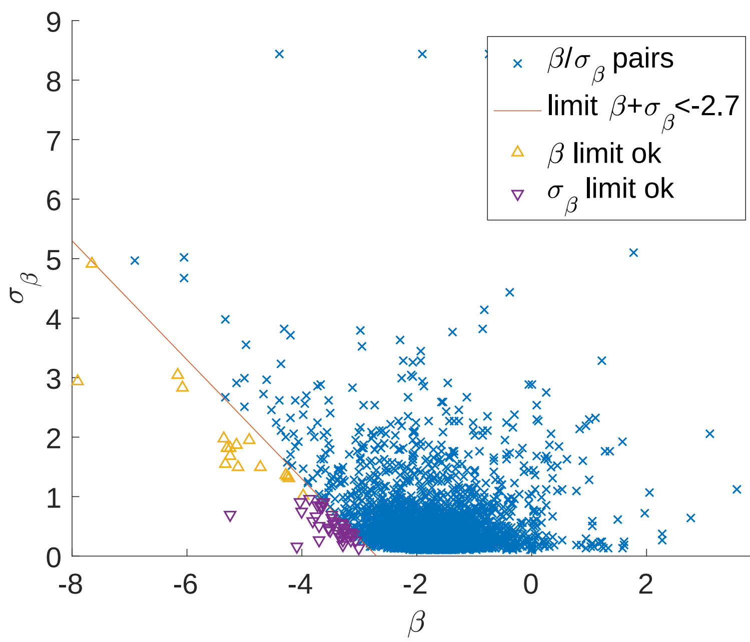


Figure 2.1.: An example of the output of the overall selection function as described in section 2.1. Here the result of using the Bouwens et al. (2014) data set as input is shown. For each galaxy, the $\beta - \sigma_\beta$ pair is plotted as a blue circle. the orange line denotes the limit $\beta + \sigma_\beta = -2.7$. Galaxies passing this selection are marked in green. Those who pass the further test $\sigma_\beta < 1$ are marked in red.

### 2.2.1. VUDS data

VUDS DR1 consists of low-resolution spectroscopic data taken in the CANDELS-COSMOS and CANDELS-ECDFS fields (Grogin et al. 2011) (Koekemoer et al. 2011). The data includes spectroscopic redshifts, one-dimensional spectra and associated physical quantities (Tasca et al. 2016). A detailed discussion can be found in the overall VUDS paper (Le Fèvre et al. 2015). The data set comes with an estimate of the reliability of the stated redshift for each object. These are named $z_{flag}$, and are tabulated in table 3 of Tasca et al. (2016). In brief, $z_{flag}$ 4 corresponds to 100% reliability, $z_{flag}$ 3 corresponds to 95-100%, $z_{flag}$ 2 indicates 70-80% and $z_{flag}$ 1 is 40-50%. $z_{flag}$ 9 indicates a spectrum in which expected key features were missing, thus the redshift was assigned based on exclusion of other solutions. There are also flags indicating the presence of an AGN, a secondary target in the slit of a primary, two line systems at different redshift as well as one indicating a physical pair. These are stated as 1X, 2X, 3X or 4X, where X is the reliability flag as discussed above. For the purposes of this work, flags 3 and 4 were chosen, allowing for combinations with the second set of flags.

### 2.2.2. Finding $\beta$

While a few physical quantities are included in VUDS DR1, $\beta$ is not among them. Hence, this needs to be calculated from the given one-dimensional spectra. Here, the definition of $\beta$ from Calzetti et al. (1994) has been used. This means a linear fit to the spectrum in the $\log F - \log \lambda$ plane, overlaid with wavelength windows to avoid stellar and interstellar absorption features.

Along with the reduced spectra, noise estimates were also published. This was taken into account via a Monte Carlo approach, in which the noise was used as weight for a randomised addition to the published spectrum. For any wavelength point $\lambda$, the calculation of the perturbed flux is as follows:

$$\tilde{F}_\lambda = F_\lambda + n_\lambda X_\lambda \tag{2.1}$$

where $F_\lambda$ is the flux of the published spectrum, $n_\lambda$ is the published noise estimate and $X_\lambda$ is a normal distributed random variable with $\mu = 0, \sigma = 1$. Thus, each $\tilde{F}_\lambda$ is drawn from a normal distribution with $\mu = F_\lambda, \sigma = n_\lambda$.

Ordering all $\tilde{F}_\lambda$ by wavelength, a new spectrum $\tilde{F}$ is obtained. $\beta$ is estimated for $\tilde{F}$ in precisely the same manner as for $F$ and the value is saved. Then the process is repeated, starting with the construction of a new $\tilde{F}$. The standard deviation of the collection of $\tilde{F}$ is then taken to be the uncertainty of the measurement of $\beta$. Each spectra thus has a best-fit value for $\beta$, as well as an estimate of the uncertainty assigned.

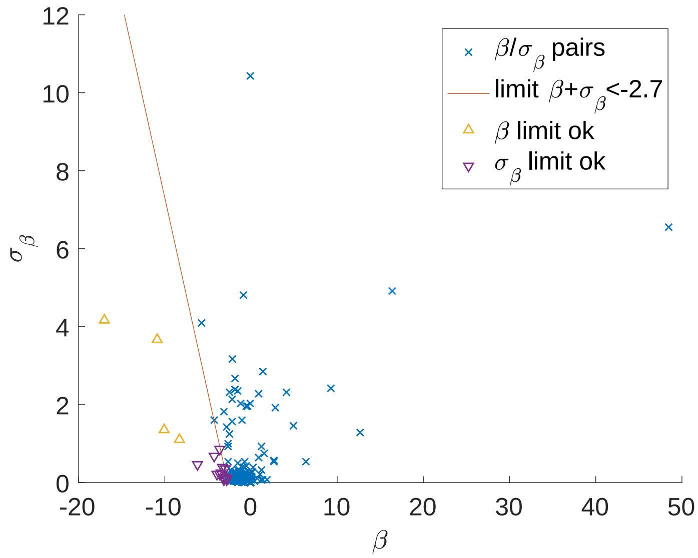


Figure 2.2.: The output of the selection function applied to the VUDS data set.

A collection of MATLAB codes for analysing the spectra can be found in appendix A.2. By running the main program, found in listing A.2, a total of 13 spectra were found to match the criteria of interesting $\beta$. Plots of the output of the selection function can be seen in fig. 2.2. This plot show that a large cluster of the galaxies have fitted $\beta$s in the range $[-2.5, -0.5]$ , which is as expected. This serves as a further sanity check on the fitting routine.

Following the automated selection, the spectra were manually examined to discard candidates where the fitting had yielded unreasonable results. Examples of this happening include when the fitting region was at the edge of observation due to redshift, or due to excessive noise. However, the selection criteria seemed robust. A few parameters of the candidates can be seen in table 2.1. An example of a spectrum including the fitted function can be seen in fig. 2.3.

## 2.3. Bouwens et al. (2014)

Bouwens et al. (2014) published an article titled "UV-continuum Slopes of >4000 z 4-8 Galaxies from the HUDF/XDF, HUDF09, ERS, CANDELS-South, and CANDELS-North Fields", which contains data suitable for this work. As stated in the title, the main result of the article was UV-continuum slopes. This makes it easy to perform cuts in the data to select suitable candidates.

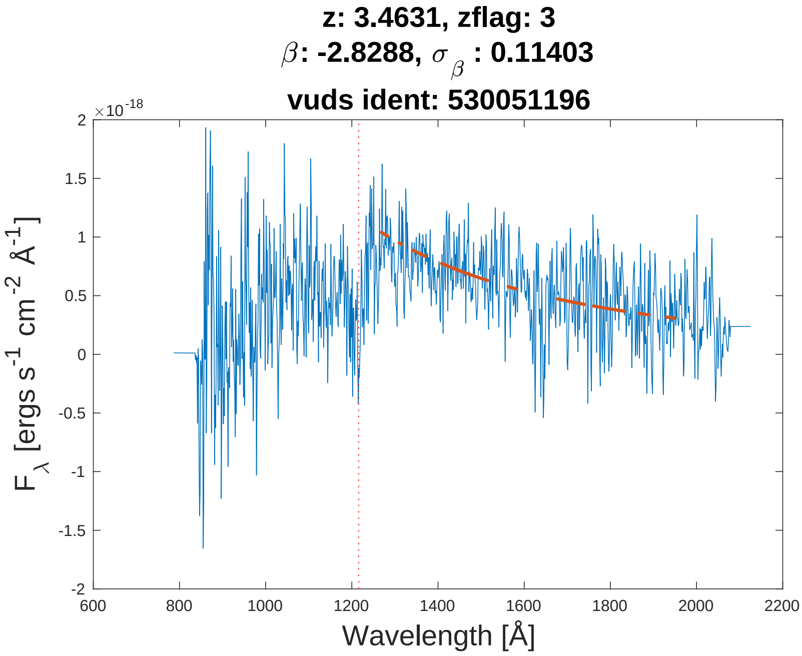


Figure 2.3.: An example of a spectrum from the VUDS data set. Wavelength is in units of Å, flux is in erg/s/cm$^2$/Å. The red lines indicate the fitted function, evaluated in the Calzetti windows. The dotted red line is placed at the wavelength of the Ly$\alpha$ -line. Z is the redshift of the object, with reliability indicator $z_{flag}$ as discussed in section 2.2. $\beta$ and $\sigma_\beta$ are described in section 2.2.2. Finally, the ID of the object in the data set is given as vuds ident.

Table 2.1.: A few parameters of the candidates from the VUDS data set. Beta is the best-fit value. Mean beta and sdev beta refer to the mean and standard deviation of the results of the Monte Carlo method. Z spec(1) is the spectroscopic redshift. Sel mag and magi refer to the selection magnitude, i band.

| beta | mean beta | sdev beta | z spec | sel mag |
|---|---|---|---|---|
| -2.8288 | -2.8001 | 0.1140 | 3.4631 | 25.1750 |
| -4.2591 | -4.1812 | 0.6901 | 0.6198 | 24.7360 |
| -6.1358 | -6.1139 | 0.4612 | 0.7621 | 24.3080 |
| -3.1378 | -3.1011 | 0.1116 | 1.2959 | 23.9380 |
| -2.9959 | -2.9183 | 0.1530 | 1.2095 | 24.8900 |

| beta | mean beta | sdev beta | z spec1 | magi |
|---|---|---|---|---|
| -3.6094 | -3.3475 | 0.2113 | 3.9900 | 24.3400 |
| -2.8847 | -2.8744 | 0.0765 | 1.1550 | 24.3920 |
| -3.3147 | -3.2625 | 0.3813 | 4.5769 | 24.0590 |
| -4.0002 | -3.9890 | 0.2043 | 0.9375 | 24.0350 |
| -3.1345 | -3.1498 | 0.0798 | 1.1292 | 24.3210 |
| -3.6005 | -3.6345 | 0.8512 | 0.8932 | 24.7480 |
| -3.0596 | -2.7430 | 0.3414 | 4.3862 | 24.7130 |
| -3.5264 | -2.8759 | 0.2316 | 4.2685 | 24.1700 |

Table 2.2.: Example data from Bouwens et al. (2014) . Table 8 in their paper. [a] The data set from which the source was selected and in which its UV-continuum slope beta derived (1=XDF, 2=HUDF09-1, 3=HUDF09-2, 4=CANDELS/ERS)

| Source ID | R.A. | Decl. | $M_{UV,AB}$ | $\beta$ | <z> | Data set[a] |
|---|---|---|---|---|---|---|
| XDF-23876748271 | 03:32:38.76 | -27:48:27.11 | -19.54 | 0.00±0.14 | 4 | 1 |

### 2.3.1. Data

The data from Bouwens et al. (2014) consists of a machine-readable table, whose overall shape can be seen in table 2.2. This matches their table 8.

### 2.3.2. Selection criteria

The selection of candidate galaxies was made using the method of section 2.1, in order to ensure fair treatment of all data sets. The selection resulted in 40 galaxies. The output of the selection function can be seen in fig. 2.4. The drawbacks of the photometric method of measuring $\beta$ can be seen in the number of galaxies with large errors. Overall, the galaxies seem to be centred at $\beta \sim -2$, which is in line with expected distributions.

Table 2.3.: Data on the object GOODSSB-25593749386 from Bouwens et al. (2014).

| | |
|---|---|
| beta | -4.04 |
| e_beta | 0.91 |
| zbin | 7 |
| Jmag | 25.502 |
| Hmag | 25.94 |

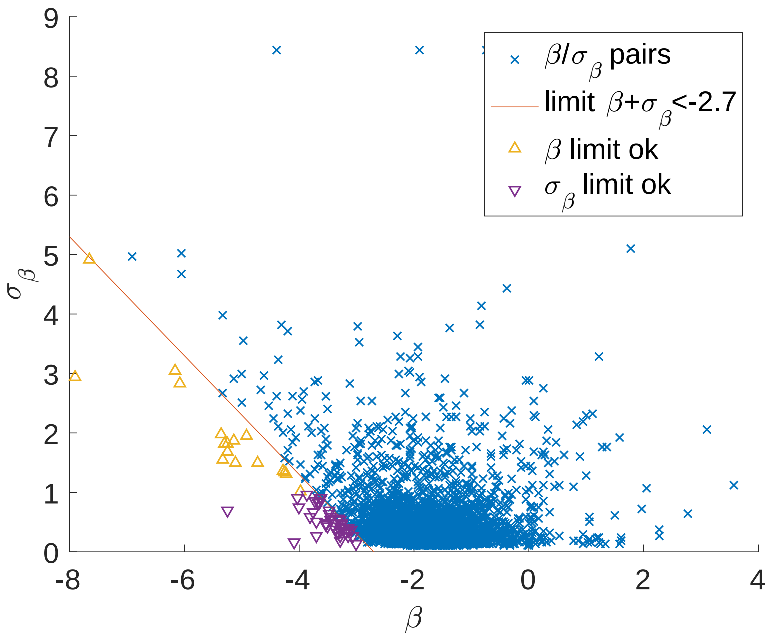


Figure 2.4.: The output of the selection function on the Bouwens et al. (2014) data set. Note the larger scatter in errors when compared to fig. 2.2.

A further selection based on luminosity was also made, since the limit for continuum spectroscopy at current telescopes is $m_{AB} \simeq 26$. Since the authors made the fluxes available in another machine-readable table, the conversion was fairly straightforward.

The final result of the selection was one object with ID GOODSSB-25593749386. This object is remarkable in that the published value for $\beta$ is $-4.04 \pm 0.91$, a selection of further information is available in table 2.3.

Matlab code for performing the selections can be found in appendix A.3. Further investigations in other data sets can be found in section 3.2.

Table 2.4.: Example data from Dunlop et al. (2013) . Table A1 in their paper.

| Name | RAJ2000 | DecJ2000 | zphot | M1500 | betaJH | $\beta_{PL} \pm 1\sigma$ |
|---|---|---|---|---|---|---|
| 'UDF12-3732-6420' | '03:32:37.32' | '-27:46:42.0' | 6.4 | -17.4 | -4 | -3.6 ± 1.5 |

## 2.4. Dunlop et al. (2013)

Using Hubble Ultra-Deep Field data, Dunlop et al. (2013) performed a measurement of $\beta$ at $z \approx 7-9$. Photometry in several bands was used to obtain $\beta$ by power-law fitting. The data was given as a table, the structure of which can be seen in table 2.4, corresponding to their table A1.

### 2.4.1. Selection

As the data was given on a form similar to that in section 2.3, the source selection is performed in the same way. MATLAB code for the analysis can be found in appendix A.4. The selection resulted in three galaxies, which have also been studied in the context of the galaxy luminosity function at z = 7–9 by McLure et al. (2013). The output of the selection function can be seen in fig. 2.5. Main features of the plot include the smaller number of galaxies, and the horizontal bands of galaxies at similar errors. The bands are likely due to rounding errors, since the $1\sigma$ values are given with only two significant digits.

The first galaxy, UDF12-4182-6112, has $\beta = -3.5 \pm 0.7$. A coordinate search in NED revealed another object of similar redshift within a small angle, most likely a second detection of the same galaxy. However, at a distance of ≈ 0.4", an object named UDFz 41826112 is located, with a stated redshift of ≈ 2.7. This distance is close to the size of the apertures used by Dunlop et al. to extract the photometry. The apparent magnitude of the object in the bands with detection is $m_{AB} \approx 28.9$ (McLure et al. 2013), outside the realm of meaningful spectroscopy. The lower-redshift object has a few photometric references, all of which also indicate AB magnitudes of $m_{AB} \approx 29$.

The second galaxy, UDF12-3973-6214, has $\beta = -3.6 \pm 0.8$. A NED search reveals that this galaxy has been studied in several surveys, and has photometry in a few bands. However, the apparent magnitude in all bands is $m_{AB} \approx 28.9$ (McLure et al. 2013) —too faint for spectroscopy.

The third galaxy, UDF12-4308-6277, has $\beta = -3.7 \pm 0.9$. Searching NED, it was discovered that this galaxy had been studied elsewhere, by McLure et al. (2013) and Schenker et al. (2014). According to McLure et al. (2013), the galaxy is at $m_{AB} \approx 29.3$, which seems too faint for meaningful spectroscopy. Schenker et al. (2014) studied the galaxy in the context

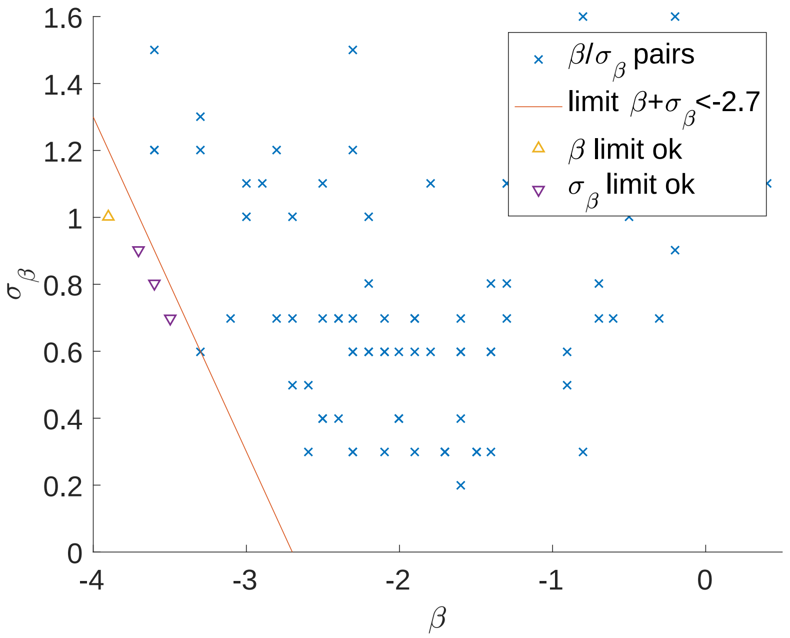


Figure 2.5.: The output of the selection function on the Dunlop et al. (2013) data set.

of Ly$\alpha$ emission by means of observations with the MOSFIRE near-infrared spectrograph, but no emission lines were found.

## 2.5. ID11

A recent article presents a possibly interesting galaxy at z = 3.12. The source is lensed by the Hubble Frontier Fields galaxy cluster AS1063 into three images. The spectra used for the article were taken over two of the images over two hours, corresponding to four hours total integration. (Vanzella et al. 2016)

Estimating $\beta$ using photometry directly (e.g. Castellano et al. 2012) was found to give $\beta = -2.95 \pm 0.12$, while SED fitting gave $\beta = -2.7 \pm 0.1$ (Vanzella et al. 2016)

Vanzella et al. claims that a single, spatially resolved region is responsible for the ultraviolet emission.

Table 2.5.: A summary of the number of candidates from each data set passing the selection criteria.

| Data set | No. of galaxies |
|---|---|
| VUDS | 13 |
| (Bouwens et al. 2014) | 1 |
| (Dunlop et al. 2013) | 0 |
| (Vanzella et al. 2016) | 1 |
| (Caminha et al. 2015) | 1 |
| **Total** | 16 |

## 2.6. Caminha et al. (2015)

As mentioned in Vanzella et al. (2016), other sources have been detected within ~100 kpc (proper) from their galaxy. One of which is a multiply-lensed Lyman-alpha blob (Caminha et al. 2015). This might be interesting, since the paper shows that it is possible to take spectra of this object, and suggests that the ionization is powered by star formation. In combination with the claims that the object is poor in dust, this indicates that the object might have an exciting value of $\beta$.

## 2.7. Summary

In table 2.5, the number of selected galaxies per data set are presented. The largest number of candidates come from the VUDS data set. This is perhaps not very surprising, since the other large data sets are photometric in nature, which makes for rather large error bars in the estimation of $\beta$. The spectroscopic nature of the VUDS data, in contrast, makes for a fairly certain determination. Further, several candidates were discarded from the photometric data sets on the basis of being too faint for spectroscopy. The VUDS data, being spectroscopic in nature, serves by itself as a confirmation that spectroscopy is possible.

For the remainder of this work, the VUDS candidates will be the main focus, since there are several of them, and the Caminha et al. (2015) and Vanzella et al. (2016) objects are already fairly well-studied.

**VUDS** Thirteen candidates of suitable quality.

**Bouwens et al. (2014)** one galaxy at $\beta = -4$, with somewhat contradictory data from Finkelstein et al. (2012).

**Dunlop et al. (2013)** Three galaxies, however all have $m_{AB} \approx 29$, which is too faint.

**Vanzella et al. (2016)** Spectra taken, beta estimated from photometry and SED fitting.

**Caminha et al. (2015)** object with spectrum, claimed to be poor in dust and having lots of star formation.

# 3. Follow-up

## 3.1. VUDS

In section 2.2, the spectra were deemed to be of sufficient quality. Hence, all candidates received follow-up investigations in public databases.

A search by coordinates revealed that SIMBAD lacked data on most of the galaxies from the ECDFS field. For the galaxies with available data, the existing data mostly amounts to a position reference and photometry. The data on the galaxies are from Capak et al. (2007) and Ilbert et al. (2013), neither of which concern themselves with the statistics of $\beta$ over the population of galaxies.

The galaxy with VUDS ID 5101244930 has also been studied in the context of spectroscopic measurements of Ly$\alpha$ equivalent width (Mallery et al. 2012). Mallery et al. (2012) selected a sample of Ly$\alpha$ emitters from the COSMOS survey, and studied them with the DEIMOS spectrograph. Mallery et al. (2012) identifies the galaxy as N7bb-77-42228, and its Ly$\alpha$ EW is stated to be $13.9^{+2.58}_{-4.88}$ Å.

For the ECDFS field, a few galaxies were found in SIMBAD, but at angular distances of 5" or more. The VUDS galaxy 530039276 had a possible match at a distance of 3."69. In combination with the differences in spectroscopically measured redshift—0.62 vs 0.44 (Cooper et al. 2012)—it seems unlikely that this refers to the same object. The VUDS galaxy 530051196 has been studied by Cameron et al. (2011), a study of galactic morphologies using near-IR data from the WFC3 on the Hubble Space Telescope.

Using the Rainbow Navigator[1], the GOODS-S and COSMOS fields were searched by coordinates for the VUDS candidates. There, postage stamp versions of available data in different bands can be seen, as well as a model SED fitted to the photometry. In general, the Rainbow Navigator showed data consistent with the VUDS spectra. However, the fitted SED requires accurate photometry. At the wavelengths covered by VUDS for these objects, several bands of photometry had rather large error bars. This means that the VUDS values for $\beta$ cannot be rejected outright on the basis of available photometry.

[1] http://rainbowx.fis.ucm.es/Rainbow_navigator_public/

Table 3.1.: A summary of the available data for the candidates from the VUDS data set. Galaxies with z ≈ 1 show the [OII]3727 line, those with z ≈ 4 show the Ly$\alpha$ line.

| VUDS-id | CANDELS-id | z | HST data | VIMOS spectrum | Chandra data |
|---|---|---|---|---|---|
| 5101001924 | 5165 | 1.155 | yes | yes | no |
| 5101227063 | 20233 | 0.8932 | yes | yes | no |
| 5101232355 | 17264 | 4.2685 | yes, smudge | yes | no |
| 5101233392 | 16301 | 0.9375 | yes | yes | no |
| 5101233724 | 16397 | 4.3862 | yes | yes | no |
| 5101244930 | 10102 | 4.5769 | yes | yes | no |
| 5101454346 | 28886 | 3.99 | yes | yes | no |
| 5101465838 | 23366 | 1.1292 | yes | yes | no |
| 530029668 | 4103 | 1.2959 | yes | yes | no |
| 530034174 | 6841 | 0.7621 | yes | yes | no |
| 530039276 | 10456 | 0.6198 | yes | yes | no |
| 530039676 | 10783 | 1.2095 | yes | yes | no |
| 530051196 | 19682 | 3.4631 | yes | yes | no |

From the Rainbow Navigator, a handy link to search NED for the object at hand was provided for each object. This revealed that the VUDS galaxies 5101001924 and 5101233392 appeared in the NEWFIRM photometric survey by Whitaker et al. (2011). Otherwise, the NED did not provide new information about the COSMOS galaxies not already known from the SIMBAD search. The ECDFS galaxies had more data available in NED, however most was photometry from various surveys (Wolf et al. 2001, Wolf et al. 2004, Grazian et al. 2006, Wuyts et al. 2008, Santini et al. 2009, Cardamone et al. 2010, Conselice et al. 2011).

The Chandra Source Catalog was also searched by coordinates in order to check for AGNs or similar possible explanations for the excessively blue values of $\beta$ found. However, this was not expected to yield any results, since the spectra had not been flagged by the VUDS team as having spectarl features indicative of AGN. The closest X-ray source to any one of the selected VUDS galaxies was $\sim 30''$ away, which does not seem to be the same object.

A summary of the literature search can be found in table 3.1.

## 3.2. Bouwens et al. (2014)

The interesting value of $\beta$ ($-4.04 \pm 0.91$) motivated a search for other published measurements of the galaxy, to check for conflicting or corroborating data. A search by

Table 3.2.: Data on the object DEEP_11281 from Finkelstein et al. (2012).

| | |
|---|---|
| beta (68 % conf. limits) | -2.74 (-2.88 -2.12) |
| z (68 % conf. limits) | 6.78 (6.48 7.01) |

coordinates in the NASA/IPAC Extragalactic Database (NED) revealed an object named SIMPLE 29289 from the Spitzer IRAC/MUSYC Public Legacy Survey in the Extended CDF-South (SIMPLE) survey (Damen et al. 2011). Using the coordinates from the NED, the object is placed $\approx 2.2''$ away from the coordinates by Bouwens et al.

The NED also provided a reference for the redshift of the object, Finkelstein et al. (2012). Searching through the dataset of Finkelstein et al. by coordinates, an object 00.0472" away from the GOODS...9386 object named DEEP_11281 was revealed, some properties of which can be seen in table 3.2.

The values of $\beta$ differ beyond the uncertainties. One possibility is that the differing values are due to the different methods the authors used in deriving $\beta$. Finkelstein et al. (2012) used SED fitting, in which synthetic spectra are calculated for galaxies with a wide range of parameters, and the best fit to photometry is chosen. The bands used in the fit of z $\approx$ 7 objects were F105W, F125W and F160W of the HST, although the authors note that $\approx$ 67 % of the objects lacked F105W -band photometry at the time of writing which may mean that this particular object is fit to merely two bands.

Bouwens et al. (2014) used a power-law fit to the available photometry, but since the GOODS...9386 object only had F125W and F160W data available, the fit is equivalent to $\beta = -2.0 + 4.39(F125W - F160W)$ (their eq. (1)). The paper by Bouwens et al. contains a section in which they compare their results to those of Finkelstein et al. (2012). That section is mainly concerned with the biases in measuring $\beta$, and suggests that Ly$\alpha$ emission may boost the F105W flux, and cause a galaxy to appear bluer for a given redshift.

Rogers et al. (2013) claim that at $6.5 < z < 7.5$, the Lyman break enters the F105W band, which may cause issues since the break may be misplaced within the filter. This may then cause the galaxy to be wrongly assigned a too low redshift, which causes problems for the SED fitting. Rogers et al. also test the effect of Ly$\alpha$ emission on simulated objects, and find that including F105W typically returns a redder colour. Indeed, Rogers et al. (2013) state that Finkelstein et al. acknowledge that the model simply breaks down at the edge of the parameter space.

Bouwens et al. (2014) is also a newer paper in which the concerns of Rogers et al. (2013) are considered, which may indicate that the bluer value of beta may be favoured. The differences in published values indicate that a spectroscopic investigation is needed, since this should be able to solve both the matter of redshift as well as $\beta$.

Table 3.3.: Coordinates of final candidates in decimal degrees (J2000), as provided by the VUDS authors (Tasca et al. 2016). GOODSSB... coordinates converted to match.

| ID | Ra | Dec |
|---|---|---|
| 5101001924 | 150.18812561 | 2.23971701 |
| 5101227063 | 150.16122437 | 2.4225471 |
| 5101232355 | 150.18969727 | 2.38568592 |
| 5101233392 | 150.14395142 | 2.37385392 |
| 5101233724 | 150.17739868 | 2.37523007 |
| 5101244930 | 150.19859314 | 2.30064392 |
| 5101454346 | 150.19970703 | 2.54534698 |
| 5101465838 | 150.1572876 | 2.46685195 |
| 530029668 | 53.22681427 | -27.87386894 |
| 530034174 | 53.04459381 | -27.84639359 |
| 530039276 | 53.02403641 | -27.8145752 |
| 530039676 | 53.03637695 | -27.81155968 |
| 530051196 | 53.01107788 | -27.74328613 |
| GOODSSB-25593749386 | 53.2330417 | -27.8273889 |

## 3.3. Summary

The location on the sky of the final candidates can be found in table 3.3. The first block of candidates at Ra $\sim$ 150 lie in the COSMOS field, others in the ECDFS field. A collection of three arcsec wide thumbnail images of the candidates can be found in appendix C.

## 3.4. X-shooter

In order to understand the underlying physics of these exciting values of $\beta$, more data is needed. This new data should preferably be spectroscopic data of higher resolution and larger wavelength range. For the photometric candidates, any spectroscopic data is better data, since this would allow for a more precise redshift determination as well as a direct measurement of $\beta$ using the Calzetti et al. (1994) windows. The spectroscopic candidates from the VUDS data set already have spectroscopy, but the VIMOS instrument is intended to be used for wide-field surveys (LeFevre et al. 2003) and has a resolution range of R $\sim 200 - 2500$. Further, the wavelength range is 3600–10000 Å—a span of 6400 Å—which is not enough to obtain data on enough spectral lines for e.g. dust or metallicity investigations. This can be seen in the spectra from this work, which contain

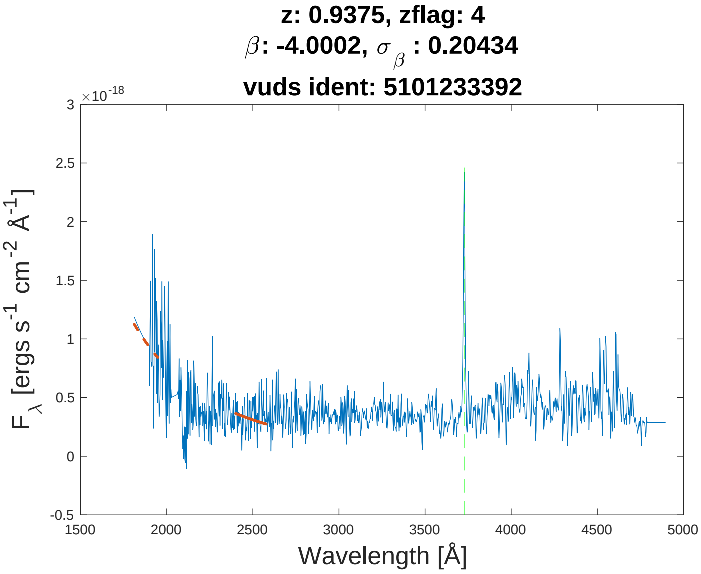


Figure 3.1.: An example of a VUDS spectrum, in which the [O II] line can be seen.

Table 3.4.: A collection of useful lines

| Line | Wavelength [Å] | Use |
|---|---|---|
| [OII] | 3727 | metallicity |
| $H_\beta$ | 4861 | dust content |
| [OIII] | 5007 | metallicity |
| $H_\alpha$ | 6563 | dust content |
| [NII] | 6548, 6584 | metallicity |

a resolved Ly$\alpha$- or [OII] line and not much else. For an example, see fig. 3.1, which shows a spectrum featuring the [O II] line and some of the Calzetti fitting windows.

A list of lines useful for dust and metallicity measurements can be found in table 3.4

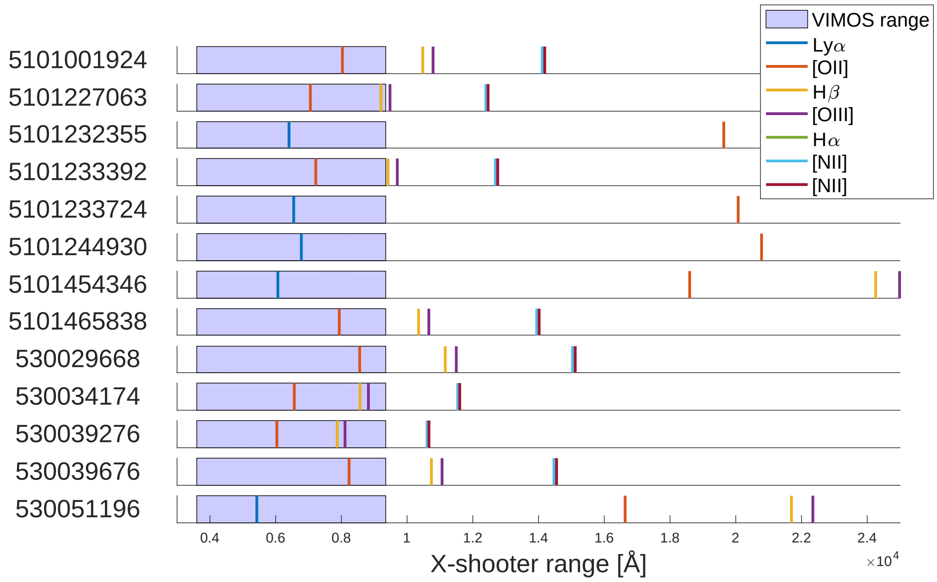


Figure 3.2.: A comparison of the X-shooter and VIMOS wavelength ranges. The x-axis covers the range of X-shooter, and the VIMOS range is indicated in blue. The rows correspond to the redshifts of the previously selected galaxies from the VUDS data set, and the VUDS ID number is stated; see table 3.1. For each redshift, a collection of interesting lines are plotted to check if they are within X-shooter range.

# 4. Conclusions

Several galaxies whose values of $\beta$ lie beyond what is easily explained by existing theory have been identified in existing data sets. Most of these have spectroscopic data available, which provides for reasonable certainty in the assessment. For now, the available data seems less than what one would want to make a certain claim of new physics, but the quality of the data at least warrants interest for further investigations. As stated in the introduction, excessively blue values of $\beta$ may indicate a population of stars of equally excessive low metallicity, whose age is very low. It may also indicate an AGN, which would explain the intense UV flux, but at least the VUDS candidates selected are tagged as not showing signs of an AGN.

The immediate next step in the follow-up of these candidates is to get hold of and re-reduce the raw data. After this, the $\beta$ fitting should be redone, and the results compared to this work. This will act as a safeguard against any hitherto unseen systematics in the original reduction pipeline. As long as the re-reduced data is in a format matching the existing data, it will be straightforward to feed it through the fitting and selection scripts of this work.

The possibility of finding several new candidates is also quite real, since the spectroscopic candidates in this work all come from the first public data release of VUDS with $\sim$ 700 galaxies. The full survey is stated to contain on the order of 10 000 galaxies with spectroscopic redshifts. (Le Fèvre et al. 2015) In this work, 13 candidates were identified out of 700. Assuming that this sample is representative for the full data set, one might therefore expect $\sim$ 180 new galaxies whose values of $\beta$ match the criteria of being deemed interesting by the standards of this work.

The suggested instrument for follow-up observations of the galaxies found in this work is X-Shooter. This is due to the much larger wavelength range, and increased resolution. There are also a few galaxies who were discarded from this study due to them having $m_{AB} > 26$, but which may be available for further study with future instruments.

## 4.1. Acknowledgements

This research has made use of the NASA/IPAC Extragalactic Database (NED) which is operated by the Jet Propulsion Laboratory, California Institute of Technology, under contract with the National Aeronautics and Space Administration.

Based on data obtained with the European Southern Observatory Very Large Telescope, Paranal, Chile, under Large Program 185.A-0791, and made available by the VUDS team at the CESAM data center, Laboratoire d'Astrophysique de Marseille, France.

This work has made use of the Rainbow Cosmological Surveys Database, which is operated by the Universidad Complutense de Madrid (UCM), partnered with the University of California Observatories at Santa Cruz (UCO/Lick,UCSC).

This work is based on observations taken by the 3D-HST Treasury Program (GO 12177 and 12328) with the NASA/ESA HST, which is operated by the Association of Universities for Research in Astronomy, Inc., under NASA contract NAS5-26555. See Brammer et al. (2012) and Skelton et al. (2014).

# Bibliography


Bouwens, R. J. et al. (2010a). "Discovery of z 8 Galaxies in the Hubble Ultra Deep Field from Ultra-Deep WFC3/IR Observations". In: *The Astrophysical Journal Letters* 709, pp. L133–L137. ISSN: 0004-637X. DOI: 10.1088/2041-8205/709/2/L133.

Bouwens, R. J. et al. (2010b). "Very Blue UV-Continuum Slope $\beta$ of Low Luminosity z 7 Galaxies from WFC3/IR: Evidence for Extremely Low Metallicities?" In: *The Astrophysical Journal Letters* 708, pp. L69–L73. ISSN: 0004-637X. DOI: 10.1088/2041-8205/708/2/L69.

Bouwens, R. J. et al. (2014). "UV-continuum Slopes of >4000 z 4-8 Galaxies from the HUDF/XDF, HUDF09, ERS, CANDELS-South, and CANDELS-North Fields". In: *The Astrophysical Journal* 793.2, p. 115. ISSN: 0004-637X. DOI: 10.1088/0004-637X/793/2/115.

Brammer, Gabriel B. et al. (2012). "3D-HST: A Wide-field Grism Spectroscopic Survey with the Hubble Space Telescope". In: *The Astrophysical Journal Supplement Series* 200, p. 13. ISSN: 0067-0049. DOI: 10.1088/0067-0049/200/2/13.

Calzetti, Daniela, Anne L. Kinney and Thaisa Storchi-Bergmann (1994). "Dust extinction of the stellar continua in starburst galaxies: The ultraviolet and optical extinction law". In: *The Astrophysical Journal* 429, pp. 582–601. ISSN: 0004-637X. DOI: 10.1086/174346.

Cameron, E. et al. (2011). "Active and Passive Galaxies at z 2: Rest-frame Optical Morphologies with WFC3". In: *The Astrophysical Journal* 743, p. 146. ISSN: 0004-637X. DOI: 10.1088/0004-637X/743/2/146.

Caminha, G. B. et al. (2015). "Discovery of a faint star-forming multiply lensed Lyman-alpha blob". In: *arXiv:1512.05655 [astro-ph]*. arXiv: 1512.05655.

Capak, P. et al. (2007). "The First Release COSMOS Optical and Near-IR Data and Catalog". In: *The Astrophysical Journal Supplement Series* 172, pp. 99–116. ISSN: 0067-0049. DOI: 10.1086/519081.

Cardamone, Carolin N. et al. (2010). "The Multiwavelength Survey by Yale-Chile (MUSYC): Deep Medium-band Optical Imaging and High-quality 32-band Photometric Redshifts in the ECDF-S". In: *The Astrophysical Journal Supplement Series* 189, pp. 270–285. ISSN: 0067-0049. DOI: 10.1088/0067-0049/189/2/270.

Castellano, M. et al. (2012). "The blue UV slopes of z 4 Lyman break galaxies: implications for the corrected star formation rate density". In: *Astronomy and Astrophysics* 540, A39. ISSN: 0004-6361. DOI: 10.1051/0004-6361/201118050.

Conselice, C. J. et al. (2011). "The Hubble Space Telescope GOODS NICMOS Survey: overview and the evolution of massive galaxies at 1.5< z< 3". In: *Monthly Notices of the*

*Royal Astronomical Society* 413, pp. 80–100. ISSN: 0035-8711. DOI: 10.1111/j.1365-2966.2010.18113.x.

Cooper, Michael C. et al. (2012). "The Arizona CDFS Environment Survey (ACES): A Magellan/IMACS Spectroscopic Survey of the Chandra Deep Field-South". In: *Monthly Notices of the Royal Astronomical Society* 425, pp. 2116–2127. ISSN: 0035-8711. DOI: 10.1111/j.1365-2966.2012.21524.x.

Damen, M. et al. (2011). "The SIMPLE Survey: Observations, Reduction, and Catalog". In: *The Astrophysical Journal* 727, p. 1. ISSN: 0004-637X. DOI: 10.1088/0004-637X/727/1/1.

Dunlop, J. S. et al. (2013). "The UV continua and inferred stellar populations of galaxies at z $\simeq$ 7-9 revealed by the Hubble Ultra-Deep Field 2012 campaign". In: *Monthly Notices of the Royal Astronomical Society* 432, pp. 3520–3533. ISSN: 0035-8711. DOI: 10.1093/mnras/stt702.

Finkelstein, Steven L. et al. (2010). "On the Stellar Populations and Evolution of Star-forming Galaxies at 6.3 $<$ z $<=$ 8.6". In: *The Astrophysical Journal* 719, pp. 1250–1273. ISSN: 0004-637X. DOI: 10.1088/0004-637X/719/2/1250.

Finkelstein, Steven L. et al. (2012). "Candels: The Evolution of Galaxy Rest-frame Ultraviolet Colors from z = 8 to 4". In: *The Astrophysical Journal* 756.2, p. 164. ISSN: 0004-637X. DOI: 10.1088/0004-637X/756/2/164.

Grazian, A. et al. (2006). "The GOODS-MUSIC sample: a multicolour catalog of near-IR selected galaxies in the GOODS-South field". In: *Astronomy and Astrophysics* 449, pp. 951–968. ISSN: 0004-6361. DOI: 10.1051/0004-6361:20053979.

Grogin, Norman A. et al. (2011). "CANDELS: The Cosmic Assembly Near-infrared Deep Extragalactic Legacy Survey". In: *The Astrophysical Journal Supplement Series* 197, p. 35. ISSN: 0067-0049. DOI: 10.1088/0067-0049/197/2/35.

Ilbert, O. et al. (2013). "Mass assembly in quiescent and star-forming galaxies since z $\simeq$ 4 from UltraVISTA". In: *Astronomy and Astrophysics* 556, A55. ISSN: 0004-6361. DOI: 10.1051/0004-6361/201321100.

Koekemoer, Anton M. et al. (2011). "CANDELS: The Cosmic Assembly Near-infrared Deep Extragalactic Legacy Survey—The Hubble Space Telescope Observations, Imaging Data Products, and Mosaics". In: *The Astrophysical Journal Supplement Series* 197, p. 36. ISSN: 0067-0049. DOI: 10.1088/0067-0049/197/2/36.

Le Fèvre, O. et al. (2015). "The VIMOS Ultra-Deep Survey: 10 000 galaxies with spectroscopic redshifts to study galaxy assembly at early epochs 2 $<$ z $\simeq$ 6". In: *Astronomy and Astrophysics* 576, A79. ISSN: 0004-6361. DOI: 10.1051/0004-6361/201423829.

LeFevre, Oliver et al. (2003). "Commissioning and performances of the VLT-VIMOS". In: vol. 4841, pp. 1670–1681. DOI: 10.1117/12.460959.

Mallery, Ryan P. et al. (2012). "Ly$\alpha$ Emission from High-redshift Sources in COSMOS". In: *The Astrophysical Journal* 760, p. 128. ISSN: 0004-637X. DOI: 10.1088/0004-637X/760/2/128.

McLure, R. J. et al. (2013). "A new multifield determination of the galaxy luminosity function at z = 7-9 incorporating the 2012 Hubble Ultra-Deep Field imaging". In:

*Monthly Notices of the Royal Astronomical Society* 432, pp. 2696–2716. ISSN: 0035-8711. DOI: 10.1093/mnras/stt627.

Meurer, Gerhardt R., Timothy M. Heckman and Daniela Calzetti (1999). "Dust Absorption and the Ultraviolet Luminosity Density at z 3 as Calibrated by Local Starburst Galaxies". In: *The Astrophysical Journal* 521, pp. 64–80. ISSN: 0004-637X. DOI: 10.1086/307523.

Reddy, N. et al. (2012). "GOODS-Herschel Measurements of the Dust Attenuation of Typical Star-forming Galaxies at High Redshift: Observations of Ultraviolet-selected Galaxies at z 2". In: *The Astrophysical Journal* 744, p. 154. ISSN: 0004-637X. DOI: 10.1088/0004-637X/744/2/154.

Rogers, A. B., R. J. McLure and J. S. Dunlop (2013). "The unbiased measurement of ultraviolet spectral slopes in low-luminosity galaxies at $z \approx 7$". In: *Monthly Notices of the Royal Astronomical Society* 429, pp. 2456–2468. ISSN: 0035-8711. DOI: 10.1093/mnras/sts515.

Santini, P. et al. (2009). "Star formation and mass assembly in high redshift galaxies". In: *Astronomy and Astrophysics* 504, pp. 751–767. ISSN: 0004-6361. DOI: 10.1051/0004-6361/200811434.

Schenker, Matthew A. et al. (2014). "Line-emitting Galaxies beyond a Redshift of 7: An Improved Method for Estimating the Evolving Neutrality of the Intergalactic Medium". In: *The Astrophysical Journal* 795, p. 20. ISSN: 0004-637X. DOI: 10.1088/0004-637X/795/1/20.

Schneider, Peter (2015). *Extragalactic Astronomy and Cosmology*. Berlin, Heidelberg: Springer Berlin Heidelberg. ISBN: 978-3-642-54082-0 978-3-642-54083-7.

Skelton, Rosalind E. et al. (2014). "3D-HST WFC3-selected Photometric Catalogs in the Five CANDELS/3D-HST Fields: Photometry, Photometric Redshifts, and Stellar Masses". In: *The Astrophysical Journal Supplement Series* 214.2, p. 24. ISSN: 0067-0049. DOI: 10.1088/0067-0049/214/2/24.

Tasca, L. A. M. et al. (2016). "The VIMOS Ultra Deep Survey First Data Release: spectra and spectroscopic redshifts of 698 objects up to z 6 in CANDELS". In: *arXiv:1602.01842 [astro-ph]*. arXiv: 1602.01842.

Vanzella, E. et al. (2016). "High-resolution spectroscopy at the faintest limits: an "ELT-like" spectrum of a young optically-thin L=0.02L* star-forming galaxy at z=3.12". In: *arXiv:1603.01616 [astro-ph]*. arXiv: 1603.01616.

Whitaker, Katherine E. et al. (2011). "The NEWFIRM Medium-band Survey: Photometric Catalogs, Redshifts, and the Bimodal Color Distribution of Galaxies out to z 3". In: *The Astrophysical Journal* 735, p. 86. ISSN: 0004-637X. DOI: 10.1088/0004-637X/735/2/86.

Wolf, C. et al. (2001). "Deep BVR photometry of the Chandra Deep Field South from the COMBO-17 survey". In: *Astronomy and Astrophysics* 377, pp. 442–449. ISSN: 0004-6361. DOI: 10.1051/0004-6361:20011142.

Wolf, C. et al. (2004). "A catalogue of the Chandra Deep Field South with multi-colour classification and photometric redshifts from COMBO-17". In: *Astronomy and Astrophysics* 421, pp. 913–936. ISSN: 0004-6361. DOI: 10.1051/0004-6361:20040525.

Wuyts, Stijn et al. (2008). "FIREWORKS U38-to-24 $\mu$m Photometry of the GOODS Chandra Deep Field-South: Multiwavelength Catalog and Total Infrared Properties of

Distant Ks-selected Galaxies". In: *The Astrophysical Journal* 682, pp. 985–1003. ISSN: 0004-637X. DOI: 10.1086/588749.

# A. Matlab code

## A.1. Overall selection method

Listing A.1: Code for making the selection of galaxies in a homogeneous manner

```
function [numcand,rows,vars] = betatable(T, name, beta, error)
% BETATABLE does cuts in large tables of betas and errors in beta
% BETATABLE(T,name, beta, error)
% the function plots beta-e_beta plane, and returns number of candidates,
% logical indices of rows and cell of variable names.

%% set limits
limit = -2.7; % safe bet to not exclude too many galaxies
e_lim = 1; % larger seems very large

%% find columns
ind_n = find(strcmp(T.Properties.VariableNames,name));
ind_b = find(strcmp(T.Properties.VariableNames,beta));
ind_e = find(strcmp(T.Properties.VariableNames,error));

%% select galaxies
% select galaxies with beta + e_beta smaller than limit (-2.7) and errors
% smaller than e_lim (1)
rows = (T.(ind_b) + T.(ind_e) < limit) & ( T.(ind_e) < e_lim);

%% select and print variables
vars={name, beta, error};

% print variables 'vars' from rows selected earlier
disp(T(rows,vars))
num = size(T(rows,vars));
numcand = num(1);

%% scatterplot beta vs e_beta
rowslim = (T.(ind_b) + T.(ind_e) < limit); % select rows only based on
    beta limit
```

```

scatter(T{~rowslim,ind_b},T{~rowslim,ind_e},'x') % all pairs outside limit
hold on % let initial scatter plot set limits of figure

xl = xlim;
% ugly hack to fix some vuds values being outside plot
if (min(T{:,ind_b}) < -10)
    xl(1) =  -20;
end
yl = ylim; % for prettifying the plot
plot(xl, (-xl+limit)) % plot line at beta + e_beta = limit

limitinds=logical(rowslim-rows);
scatter(T{limitinds,ind_b},T{limitinds, ind_e},'^') % under limit
scatter(T{rows,ind_b},T{rows, ind_e},'v') % also under error limit

axis([xl(1), xl(2), 0, yl(2)]); % skip negative parts of line
xlabel('\beta', 'FontSize', 18)
ylabel('\sigma_\beta', 'FontSize', 18)
% colors are wrong in legend, known bug (1283854) in matlab R2015b, fixed
% in R2016a
set(gca,  'FontSize', 18)
legend({'\beta/\sigma_\beta pairs', 'limit \beta+\sigma_\beta<-2.7', '\
    beta limit ok', '\sigma_\beta limit ok'}, 'FontSize', 18)
hold off
```

## A.2. VUDS spectra

Listing A.2: Code for evaluating and plotting spectra with interesting $\beta$

```
%% vuds betas
% using the spectra found in the ecdfs and cosmos fields of the vimos
% ultra-deep survey. This program is intended to find interesting betas,
% and examine the spectra to see if any are worthy of follow-up.

%% lines of interest
lya = 1216;
oii = 3727;

%% Find betas
tic;
vudsloop_ecdfs;
```

```
toc
tic;
vudsloop_cosmos;
toc

%% use betatable function for homogeneous cuts in data
Tvudsecd = array2table([vuds_ident, Beta_ecdfs(:,1:2)], 'VariableNames',{'
    ID','beta','std_beta'});
Tvudscos = array2table([vuds_ident1, Beta_cosmos(:,1:2)], 'VariableNames'
    ,{'ID','beta','std_beta'});

[necd, recd, vecd] = betatable(Tvudsecd, 'ID', 'beta', 'std_beta');
figure
[ncos, rcos, vcos] = betatable(Tvudscos, 'ID', 'beta', 'std_beta');
figure
%% indices for plotting
ind_ecdfs = find(recd > 0);
ind_cosmos = find(rcos > 0);

%% list betas of interesting spectra
disp('ecdfs')
disp('    beta       z')
list_ecdfs = [Beta_ecdfs(ind_ecdfs,1), z_spec(ind_ecdfs)];
disp(list_ecdfs)

disp('cosmos')
disp('    beta       z')
list_cosmos = [Beta_cosmos(ind_cosmos,1), z_spec1(ind_cosmos)];
disp(list_cosmos)

%% plot spectra to check for dumbness
% ecdfs
for i = 1:necd
    j = ind_ecdfs(i);
    fpath = '../data/cesam_VUDS-DR1_spectra_2016-02-09T123900Z/VUDS-ECDFS-
        DR1/spec1d/';

    %% find spectra
    [spec,lambda_rest] = vudsspec(fpath, vuds_ident(j), z_spec(j));

    %% indices for fitted function
    [~, ~, specind] = windind(lambda_rest, spec);

    %% plot spectrum
```

```
    % fitted function
    func=10.^(Beta_ecdfs(j,1).*log10(lambda_rest(specind)) + Beta_ecdfs(j,3));

    plot(lambda_rest, spec);
    title({strcat('i = ', num2str(j), ', z = ', num2str(z_spec(j))), ...
        strcat('Beta = ', num2str(Beta_ecdfs(j,1)), ', std beta = ', num2str(Beta_ecdfs(j,2))), ...
        strcat('vuds ident: ', num2str(vuds_ident(j)))});

    hold on
    plot(lambda_rest(specind),func,'.')
    hold off

    plotlines(lya,oii)
end

% cosmos
for i = 1:ncos
    j = ind_cosmos(i);
    fpath = '../data/cesam_VUDS-DR1_spectra_2016-02-09T123900Z/VUDS-COSMOS-DR1/spec1d/';

    %% find spectra
    [spec,lambda_rest] = vudsspec(fpath, vuds_ident1(j), z_spec1(j));

    %% indices for fitted function
    [~, ~, specind] = windind(lambda_rest, spec);

    %% plot spectrum
    % fitted function
    func=10.^(Beta_cosmos(j,1).*log10(lambda_rest(specind)) + Beta_cosmos(j,3));

    plot(lambda_rest, spec);
    title({strcat('i = ', num2str(j), ', z = ', num2str(z_spec1(j))), ...
        strcat('Beta = ', num2str(Beta_cosmos(j,1)), ', std beta = ', num2str(Beta_cosmos(j,2))), ...
        strcat('vuds ident: ', num2str(vuds_ident1(j)))});

    hold on
    plot(lambda_rest(specind),func,'.')
    hold off

```

```
    plotlines(lya,oii)
end
```

Listing A.3: Code for calculating $\beta$ for spectra in ECDFS field

```
%% vuds dr1, batch mode. ecfds field
% intention: find beta from the spectroscopic survey VUDS.
% 1d spectra from 3600 to 9350Å
% FITS keywords: http://heasarc.gsfc.nasa.gov/docs/fcg/standard_dict.html

% location of spectra
fpath = '../data/cesam_VUDS-DR1_spectra_2016-02-09T123900Z/VUDS-ECDFS-DR1/spec1d/';
% location of noise
npath = '../data/cesam_VUDS-DR1_spectra_2016-02-09T123900Z/VUDS-ECDFS-DR1/spec1dnoise/';

%% find z
% z_spec is tabulated in the text file
% cesam_vuds_spectra_dr1_ecdfs_catalog_1455020359.txt
read_vuds_ecdfs;
% now z is found in z_spec

%% check reliability of z
% discard z with low reliability, keep zflags 3 or 4
zf=[3 4 13 14 23 24 33 34 43 44];

%% preallocate
Beta_ecdfs = zeros(length(z_spec),5);

%% loop over all spectra
parfor i=1:length(z_spec)
    %% exclude spectra with problems
    % skip object 4 in z_spec list, sice fits file is missing.
    % if z_spec is smaller than z_min, Calzetti's windows are bluewards of
    % the observed spectrum
    % in order to fit last window, z_min needs to be crval/2400 - 1 which
    % is roughly 0.4628, hence all z < 0.4628 can be excluded
    % indices 94, 189, 190, 208, 259 are missing keywords and thus excluded
    % index 219 is excluded since all elements are identically zero
    % use only spectra with ok zflags
    if (i~=4 && i~=94 && i~=189 && i~=190 && i~=208 && i~=219 && i~=259 && z_spec(i)>0.4628 && any(zflags(i)==zf))
```

```
        %% find spectrum
        [spec, lambda_rest] = vudsspec(fpath, vuds_ident(i), z_spec(i));
        [noise, noiselambda_rest] = vudsspec(npath, vuds_ident(i), z_spec(i));

        % discard flat ends of spectra, [20 1080] looks decent when
        % plotting all
        spec = spec(20:1080);
        lambda_rest = lambda_rest(20:1080);
        noise = noise(20:1080);
        noiselambda_rest = noiselambda_rest(20:1080);

        %% find calzetti windows
        % note: want indices from flux > 0, by indexing all with this,
        % problems of differing length are avoided
        [tw, tf, specind] = windind(lambda_rest, spec);
        [ntw, ntf, ~] = windind(noiselambda_rest, noise);

        %% Fit to data
        f = fit(log10(lambda_rest(specind))',log10(spec(specind))','poly1');

        n = 500; % number of iterations
        fvec = zeros(n,2);
        l = length(spec(specind));
        spi = spec(specind);
        noi = noise(specind);
        sli = lambda_rest(specind);
        for j = 1:n
            randspec = spi + randn(1,l) .* noi;
            [~,~,randind]=windind(sli,randspec);
            rf = fit(log10(sli(randind))',log10(randspec(randind))','poly1');
            fvec(j,:) = [rf.p1 rf.p2];
        end

        %% Fill vector of galaxies
        % columns: best fit beta, std_beta, best fit 2nd term, mean
        % beta, mean 2nd term
        Beta_ecdfs(i,:) = [f.p1, std(fvec(:,1)), f.p2, mean(fvec(:,1)), mean(fvec(:,2))];

    end

```

```
end
```

Listing A.4: Code for calculating $\beta$ for spectra in COSMOS field

```
%% vuds dr1, batch mode. cosmos field
% intention: find beta from the spectroscopic survey VUDS.
% 1d spectra from 3600 to 9350Å
% FITS keywords: http://heasarc.gsfc.nasa.gov/docs/fcg/standard_dict.html

% location of spectra
fpath = '../data/cesam_VUDS-DR1_spectra_2016-02-09T123900Z/VUDS-COSMOS-DR1/spec1d/';
% location of noise
npath = '../data/cesam_VUDS-DR1_spectra_2016-02-09T123900Z/VUDS-COSMOS-DR1/spec1dnoise/';

%% find z
% z_spec is tabulated in the text file
% cesam_vuds_spectra_dr1_cosmos_catalog_1455616732.txt
read_vuds_cosmos;
% now z is found in z_spec1

%% check reliability of z
% discard z with low reliability, keep zflags 3 or 4
zf=[3 4 13 14 23 24 33 34 43 44];

%% preallocate
Beta_cosmos = zeros(length(z_spec1),5);

%% loop over all spectra
parfor i=1:length(z_spec1)
    %% exclude spectra with problems
    % if z_spec is smaller than z_min, Calzetti's windows are bluewards of
    % the observed spectrum
    % in order to fit last window, z_min needs to be crval/2400 - 1 which
    % is roughly 0.4628, hence all z < 0.4628 can be excluded
    % index 85 is missing crval1 keyword, excluded
    % use only spectra with ok zflags
    if (i~=85 && z_spec1(i)>0.4628 && any(zflags1(i)==zf))
        %% find spectrum
        [spec, lambda_rest] = vudsspec(fpath, vuds_ident1(i), z_spec1(i));
        [noise, noiselambda_rest] = vudsspec(npath, vuds_ident1(i), z_spec1(i));

```

```
        % discard flat ends of spectra, [20 1080] looks decent when
        % plotting all
        spec = spec(20:1080);
        lambda_rest = lambda_rest(20:1080);
        noise = noise(20:1080);
        noiselambda_rest = noiselambda_rest(20:1080);

        %% find calzetti windows
        % note: want indices from flux > 0, by indexing all with this,
        % problems of differing length are avoided
        [tw, tf, specind] = windind(lambda_rest, spec);
        [ntw, ntf, ~] = windind(noiselambda_rest, noise);

        if (length(spec(specind)) > 1)
            %% Fit to data
            f = fit(log10(lambda_rest(specind))',log10(spec(specind))','
                poly1');

            n = 500; % number of iterations
            fvec = zeros(n,2);
            l = length(spec(specind));
            spi = spec(specind);
            noi = noise(specind);
            sli = lambda_rest(specind);
            for j = 1:n
                randspec = spi + randn(1,l) .* noi;
                [~,~,randind]=windind(sli,randspec);
                rf = fit(log10(sli(randind))',log10(randspec(randind))','
                    poly1');
                fvec(j,:) = [rf.p1 rf.p2];
            end

            %% Fill vector of galaxies
            % columns: best fit beta, std_beta, best fit 2nd term, mean
            % beta, mean 2nd term
            Beta_cosmos(i,:)=[f.p1, std(fvec(:,1)), f.p2, mean(fvec(:,1)),
                 mean(fvec(:,2))];
        end
    end

end
```

Listing A.5: Function for highlighting Ly$\alpha$ and OII lines

```
function plotlines(lya, oii)
% PLOTLINES plots the lya and oii lines
% PLOTLINES(lya, oii)

xl = xlim;
hold on
if (lya>xl(1) && lya<xl(2))
    plot([lya lya], ylim,':r')
end
if (oii>xl(1) && oii<xl(2))
    plot([oii oii],ylim,'—g')
end
hold off
```

## A.3. Bouwens et al. 2014

Listing A.6: Code for making a selection of, and plotting galaxies from Bouwens et al. 2014

```
%% plot data from Bouwens et al. 2014
% data is read using the script readbouwens2014, and later plotted.
% fields used: HUDF/XDF HUDF09, ERS, CANDELS—SOUTH, CANDELS—NORTH
%
% curly braces give values instead of smaller table, for example:
% beta_eb = T{rows, {'beta','e_beta'}}; gives a (many)x2 matrix, useful
    for
% plotting
%% Read data
readbouwens2014;

% read flux data
readbouwensfluxes2014;

%% find duplicates
[~, uniqueIdx] =unique(apj500457t8mrt.ID);  % indices of unique rows
T8 = apj500457t8mrt(uniqueIdx,:); % select only unique

% same for table of fluxes
[~, uniqueIdx] =unique(apj500457t9mrt.ID);
T9 = apj500457t9mrt(uniqueIdx,:);

%% join tables
```

```
Tbouw = join(T8,T9);

%% calculate magnitudes in AB system, following Oke 1983
% AB = −2.5log10(f_nu) +48.60, f_nu is in erg s^−1 cm^−2 Hz^?1
% 1 Jy = 10^−23 erg s^−1 cm^−2 Hz^?1
% −2.5*log10(1/(3631e−23)) = −48.6
% with f in Jy, m_AB = −2.5log10(f/3631 Jy) (monochromatic)
% values are given in 100 pJy = 10^−10 Jy
% calculation the goes as m_AB = −2.5 * log10(flux *10^−10 /3631)
% m_ab = −2.5 *( log10(flux) −10 −3.56)
% note: columns in T9 ordered by wavelength
mags = {'imag', 'Imag', 'zmag', 'ymag', 'Ymag', 'Jmag', 'JHmag', 'Hmag'};
bands = {'iflux', 'Iflux', 'zflux', 'yflux', 'Yflux', 'Jflux', 'JHflux', '
    Hflux'};
Tmag=array2table(−2.5.*( log10(Tbouw{:,bands}) −13.56), 'VariableNames',
    mags);

bluestband = cell(size(Tbouw,1),1);
bluestmag  = zeros(size(Tbouw,1),1);
for ii = 1:size(Tmag,1)
    jj = find(~ismissing(Tmag(ii,mags)),1); % works per row
    bluestband(ii) = mags(jj);
    bluestmag(ii) = Tmag{ii,mags(jj)};

end

Tmag.bluestband = bluestband;
Tmag.bluestmag = bluestmag;

%% merge tables
Tbouw =[Tbouw Tmag];

%% find candidates
[ncand,rows,vars]=betatable(Tbouw,'ID','beta','e_beta');

Tbouw(rows,vars)
ncand

%% scatterplot mag − beta
scatter(Tbouw.bluestmag, Tbouw.beta);
hold on
scatter(Tbouw.bluestmag(rows), Tbouw.beta(rows), 'r+')
hold off
```

```
%% scatter3
scatter3(Tbouw.bluestmag, Tbouw.beta, Tbouw.e_beta); xlabel('mag');ylabel(
    'beta');zlabel('eb');
hold on
scatter3(Tbouw.bluestmag(rows), Tbouw.beta(rows), Tbouw.e_beta(rows), 'r+'
    )

%% find the mostest interestingest object
r=strcmp(Tbouw.ID,'GOODSSB-25593749386');
Tbouw(r,:)
```

## A.4. Dunlop et al. 2013

Listing A.7: Code for making a selection of, and plotting galaxies from Dunlop et al. 2013

```
%% plot data from Dunlop et al. 2013
% data is read using the script readdunlop2013, and later plotted.
%
% curly braces give values instead of smaller table, for example:
% beta_eb = T{rows, {'beta','e_beta'}}; gives a (many)x2 matrix, useful
    for
% plotting
%% Read data
readdunlop2013;

%% find candidates
[ncand,rows,vars]=betatable(adunlop2013,'Name','betaPL','sigma');

adunlop2013(rows,vars)
ncand
```

# B. VUDS candidate data

## B.1. SIMBAD

**5101001924** http://simbad.u-strasbg.fr/simbad/sim-id?Ident=%404326855

**5101227063** http://simbad.u-strasbg.fr/simbad/sim-id?Ident=%404362019

**5101232355** http://simbad.u-strasbg.fr/simbad/sim-id?Ident=%404362895

**5101233392** http://simbad.u-strasbg.fr/simbad/sim-id?Ident=%4010027656

**5101233724** http://simbad.u-strasbg.fr/simbad/sim-id?Ident=%404363174

**5101244930** http://simbad.u-strasbg.fr/simbad/sim-id?Ident=%404365043

**5101454346** http://simbad.u-strasbg.fr/simbad/sim-id?Ident=%404459809

**5101465838** http://simbad.u-strasbg.fr/simbad/sim-id?Ident=%404461756

**530029668** no match

**530034174** no match

**530039276** no match

**530039676** 3."69 match http://simbad.u-strasbg.fr/simbad/sim-id?Ident=%406293247

**530051196** http://simbad.u-strasbg.fr/simbad/sim-id?Ident=%408406763

## B.2. Candidate spectra

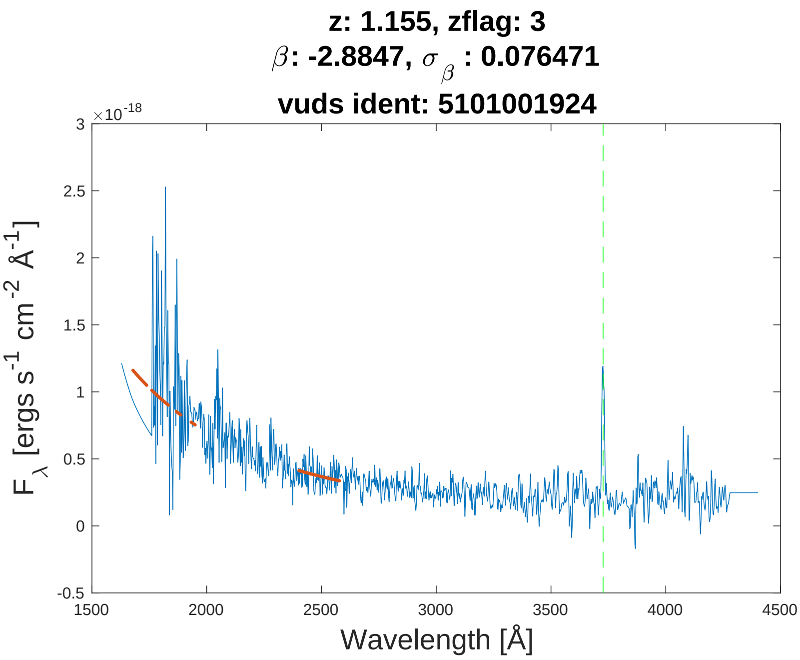
z: 1.155, zflag: 3
β: -2.8847, σβ : 0.076471
vuds ident: 5101001924
×10-18
Fλ [ergs s-1 cm-2 Å-1]
Wavelength [Å]

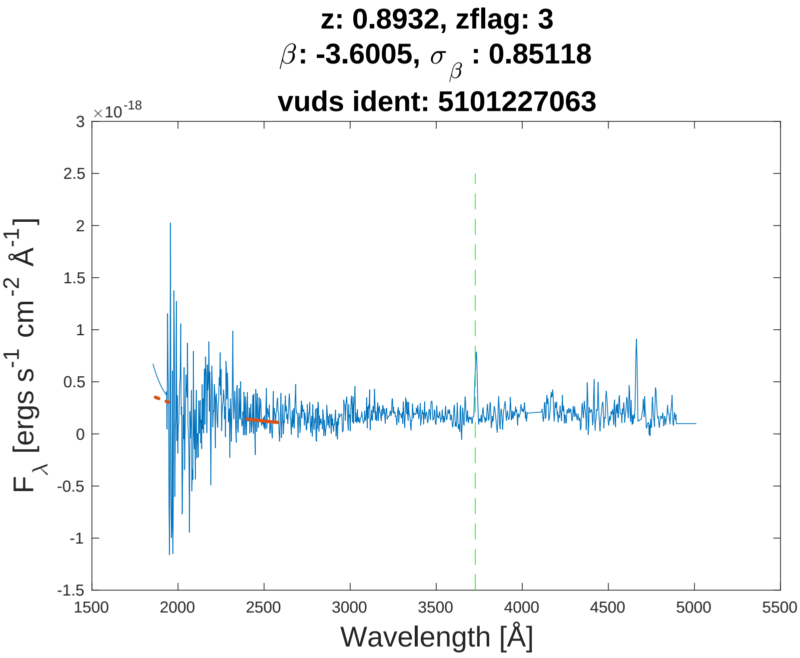
z: 0.8932, zflag: 3
β: -3.6005, σβ : 0.85118
vuds ident: 5101227063
×10-18
Fλ [ergs s-1 cm-2 Å-1]
Wavelength [Å]

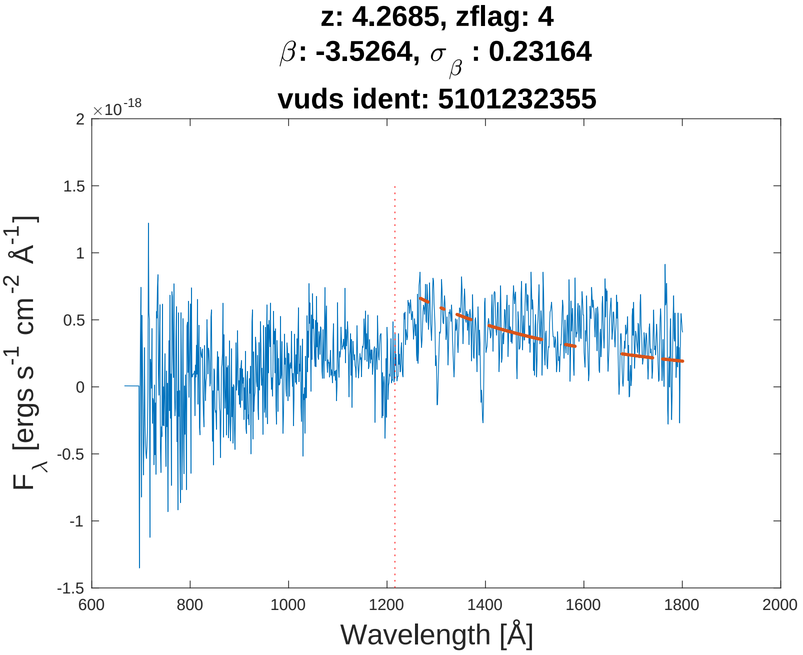
z: 4.2685, zflag: 4
β: -3.5264, σ β : 0.23164
vuds ident: 5101232355
×10^-18
F λ [ergs s^-1 cm^-2 Å^-1]
Wavelength [Å]

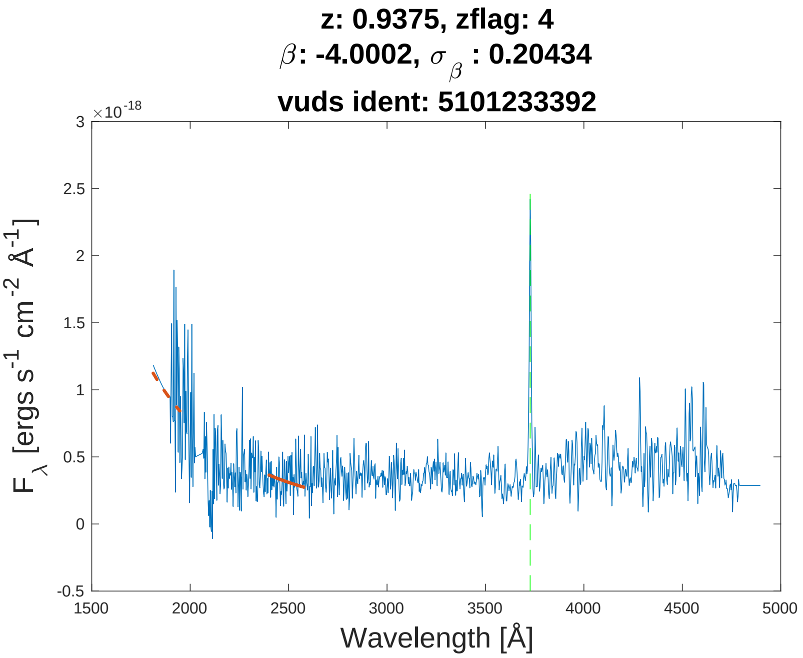
z: 0.9375, zflag: 4
β: -4.0002, σ β : 0.20434
vuds ident: 5101233392
×10^-18
F λ [ergs s^-1 cm^-2 Å^-1]
Wavelength [Å]

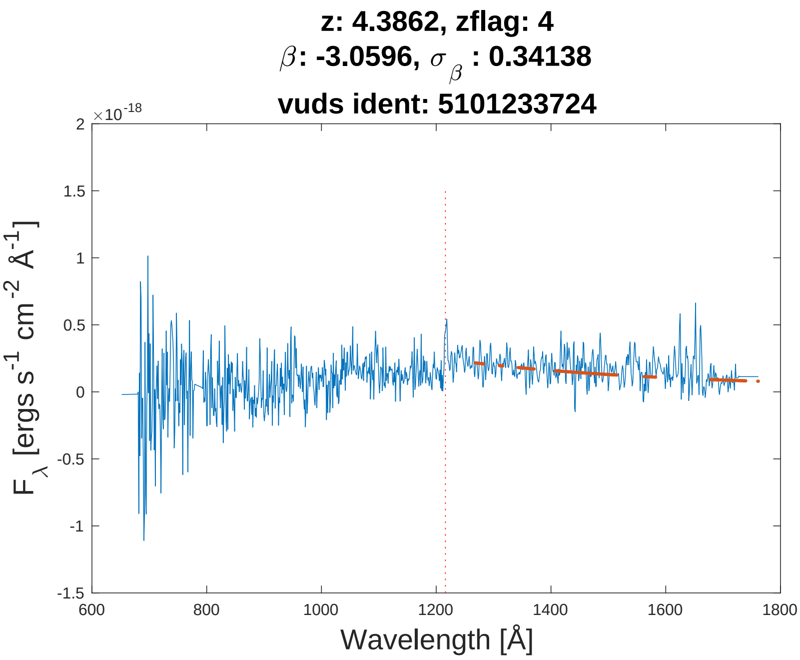
z: 4.3862, zflag: 4
β: -3.0596, σ β : 0.34138
vuds ident: 5101233724
×10^-18
F_λ [ergs s^-1 cm^-2 Å^-1]
Wavelength [Å]

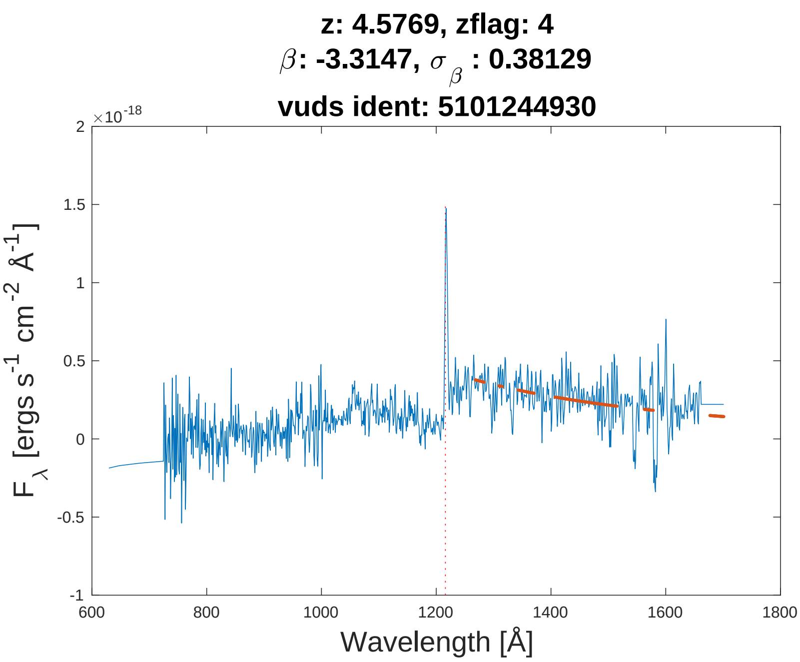
z: 4.5769, zflag: 4
β: -3.3147, σ β : 0.38129
vuds ident: 5101244930
×10^-18
F_λ [ergs s^-1 cm^-2 Å^-1]
Wavelength [Å]

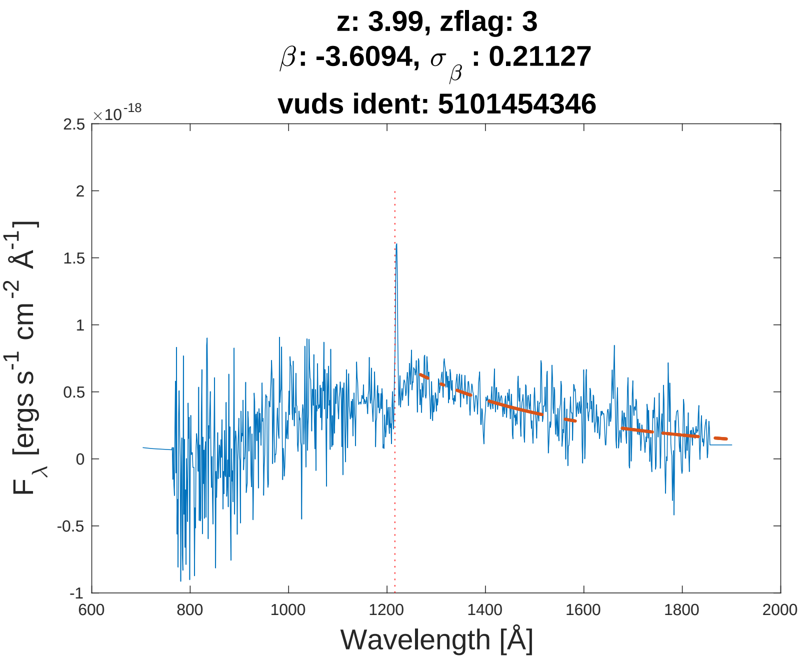
z: 3.99, zflag: 3
β: -3.6094, σ_β : 0.21127
vuds ident: 5101454346
×10^-18
F_λ [ergs s^-1 cm^-2 Å^-1]
Wavelength [Å]

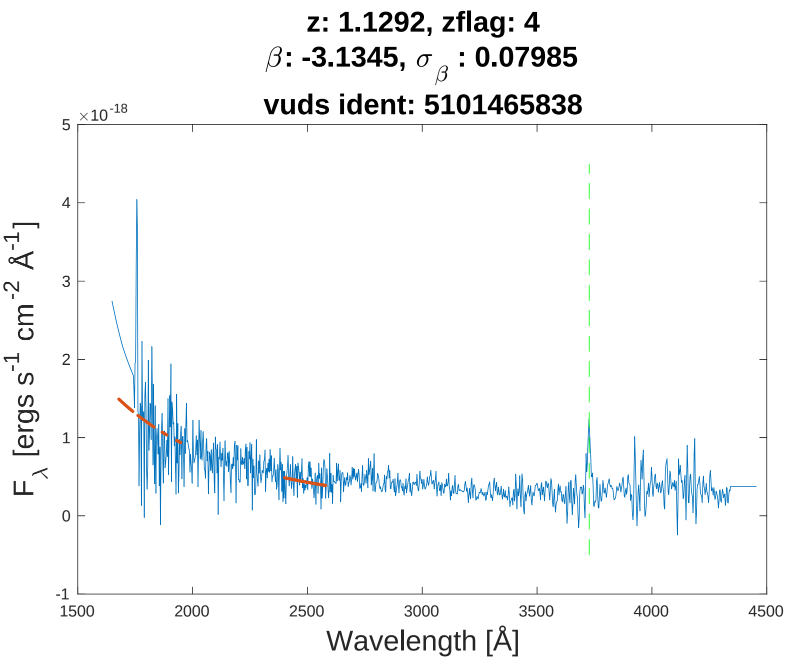
z: 1.1292, zflag: 4
β: -3.1345, σ_β : 0.07985
vuds ident: 5101465838
×10^-18
F_λ [ergs s^-1 cm^-2 Å^-1]
Wavelength [Å]

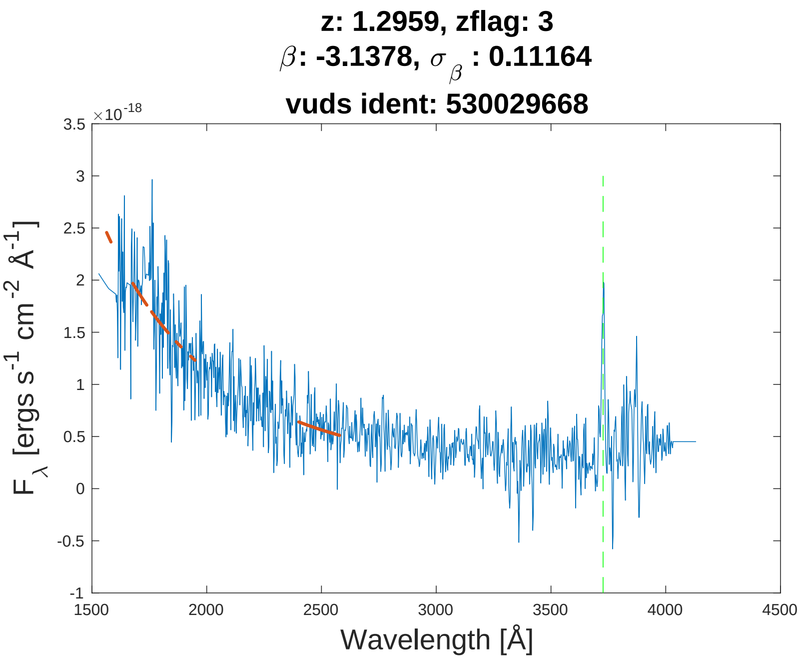
z: 1.2959, zflag: 3
β: -3.1378, σ β : 0.11164
vuds ident: 530029668
×10-18
Fλ [ergs s-1 cm-2 Å-1]
Wavelength [Å]

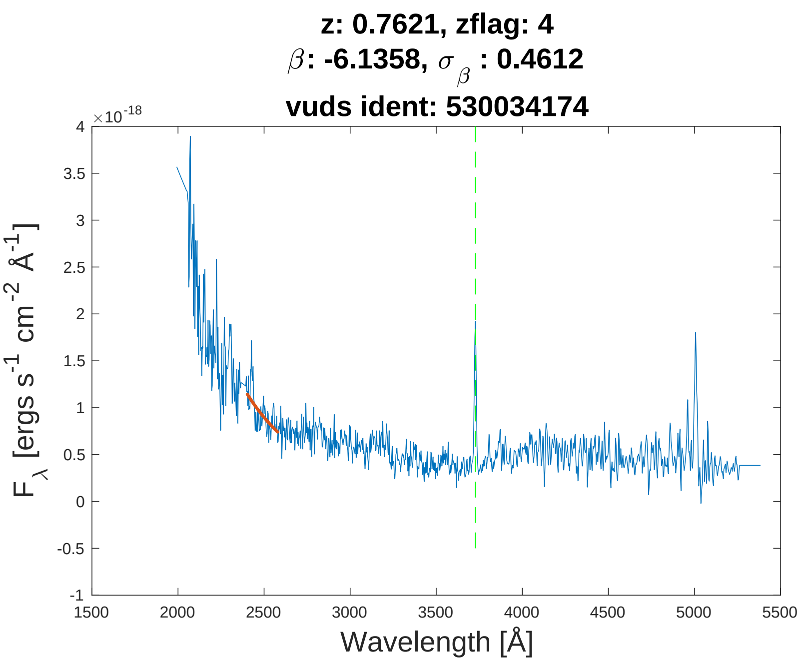
z: 0.7621, zflag: 4
β: -6.1358, σ β : 0.4612
vuds ident: 530034174
×10-18
Fλ [ergs s-1 cm-2 Å-1]
Wavelength [Å]

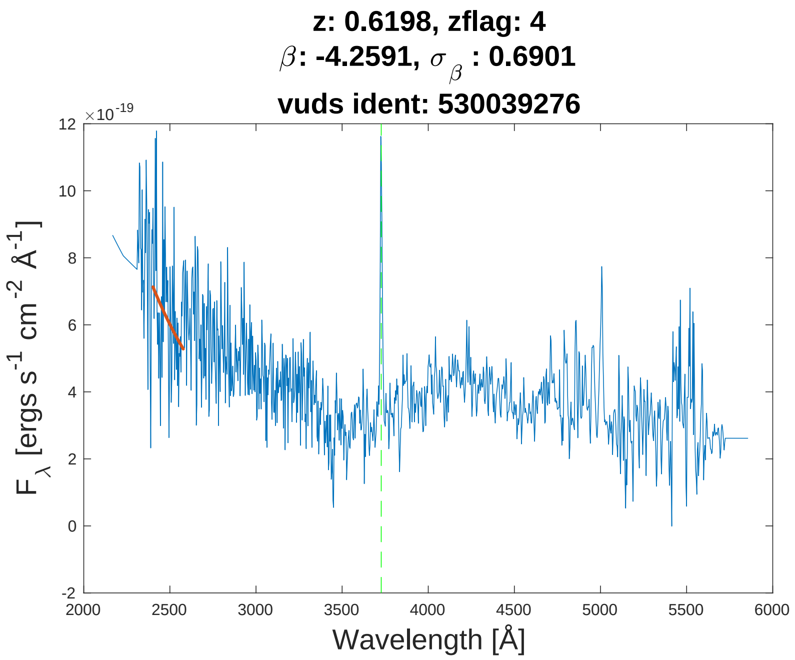
z: 0.6198, zflag: 4
β: -4.2591, σ β : 0.6901
vuds ident: 530039276
×10^-19
F λ [ergs s^-1 cm^-2 Å^-1]
Wavelength [Å]
12
10
8
6
4
2
0
-2
2000
2500
3000
3500
4000
4500
5000
5500
6000

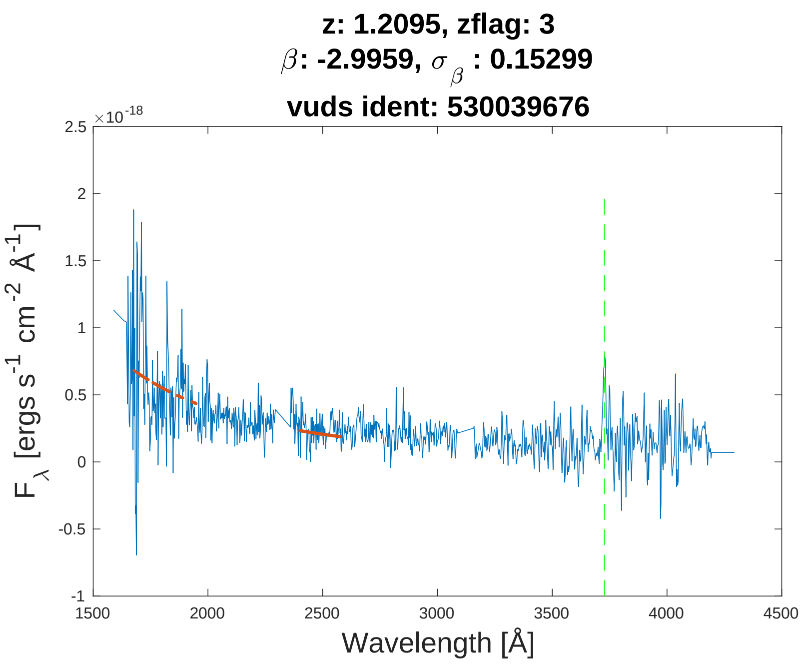
z: 1.2095, zflag: 3
β: -2.9959, σ β : 0.15299
vuds ident: 530039676
×10^-18
F λ [ergs s^-1 cm^-2 Å^-1]
Wavelength [Å]
2.5
2
1.5
1
0.5
0
-0.5
-1
1500
2000
2500
3000
3500
4000
4500

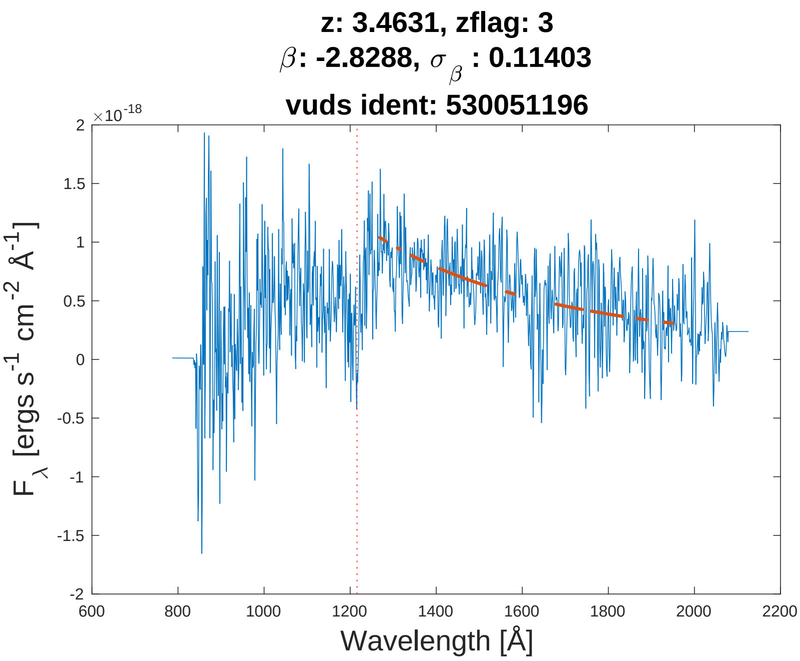
z: 3.4631, zflag: 3
β: -2.8288, σ β : 0.11403
vuds ident: 530051196
×10^-18
F λ [ergs s^-1 cm^-2 Å^-1]
Wavelength [Å]
2
1.5
1
0.5
0
-0.5
-1
-1.5
-2
600
800
1000
1200
1400
1600
1800
2000
2200

# C. Thumbnail images of candidates

These images are taken from the F125W+F140W+F160W detection mosaics from the 3DHST survey, publicly available at `http://3dhst.research.yale.edu/Data.php`. For further reference, see Brammer et al. (2012), Skelton et al. (2014), Grogin et al. (2011) and Koekemoer et al. (2011). The thumbnails are three arcsec in both width and height, and are centred on the coordinates of table 3.3.

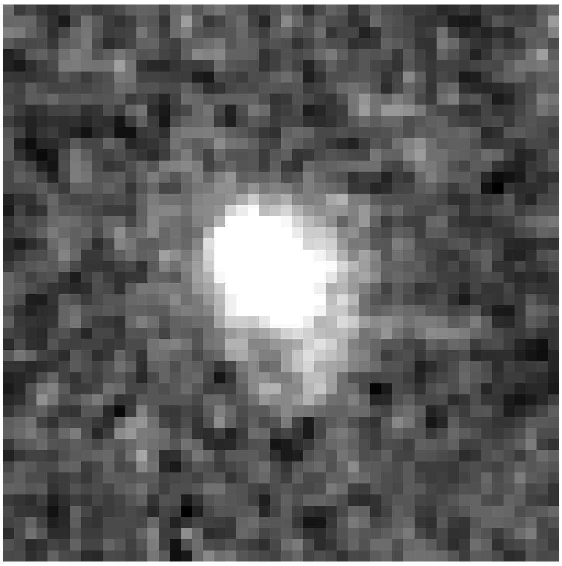

Figure C.1.: 5101001924

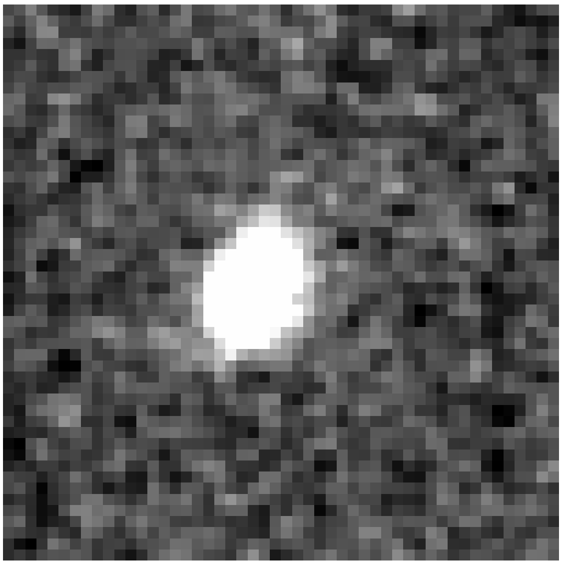

Figure C.2.: 5101227063

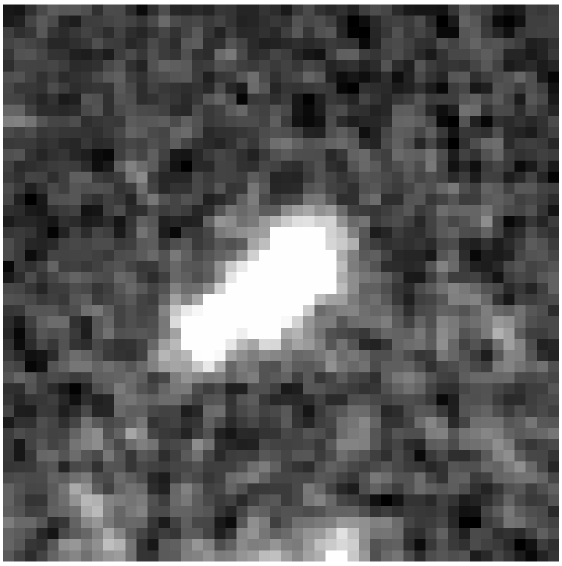

Figure C.3.: 5101232355

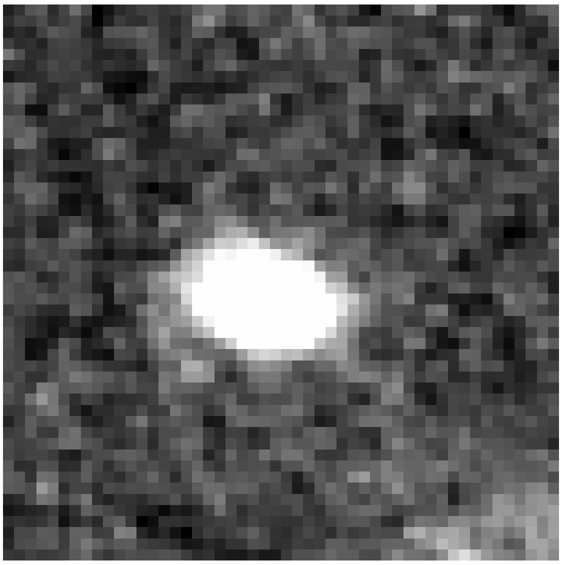

Figure C.4.: 5101233392

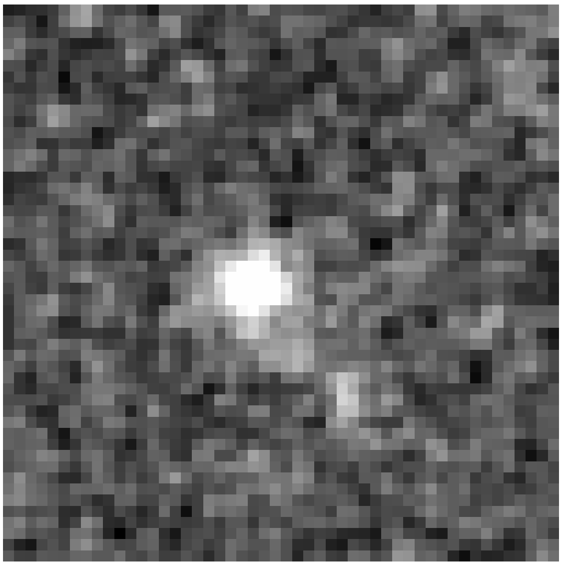

Figure C.5.: 5101233724

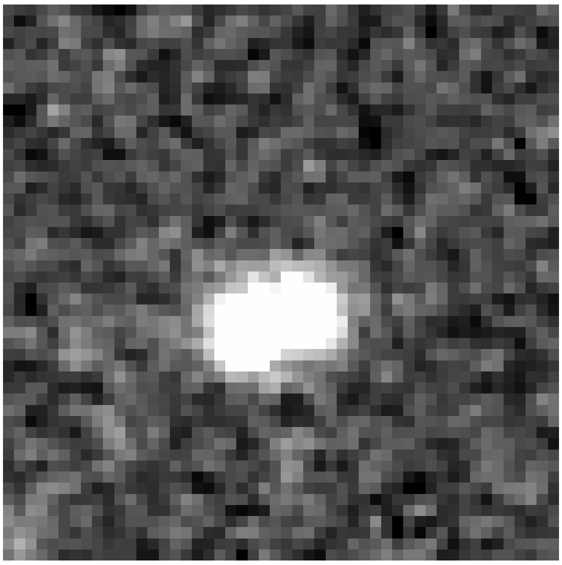

Figure C.6.: 5101244930

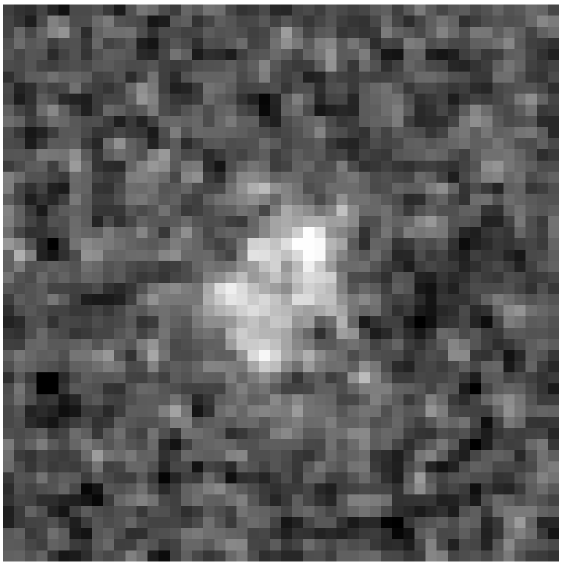

Figure C.7.: 5101454346

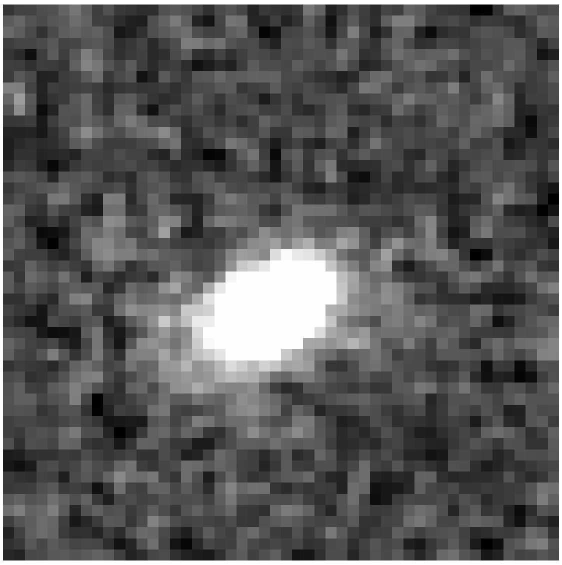

Figure C.8.: 5101465838

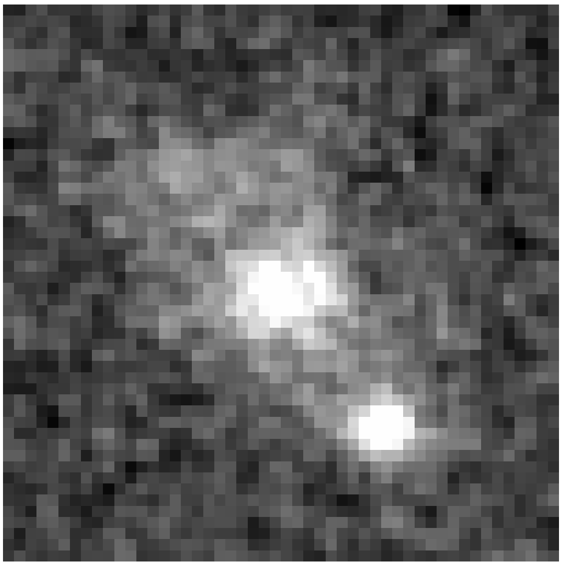

Figure C.9.: 530029668

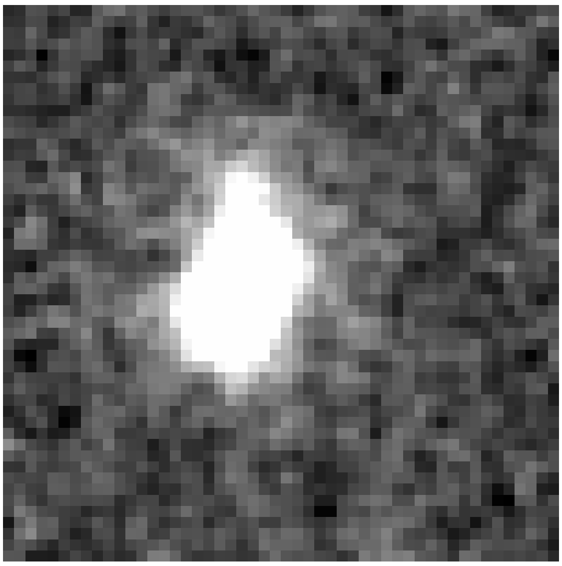

Figure C.10.: 530034174

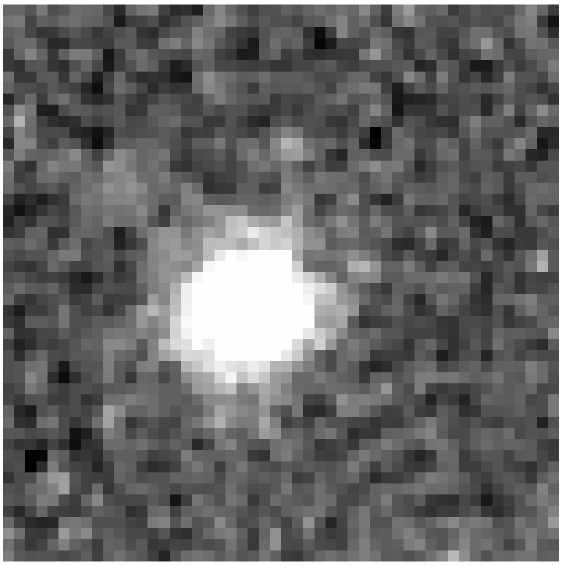

Figure C.11.: 530039276

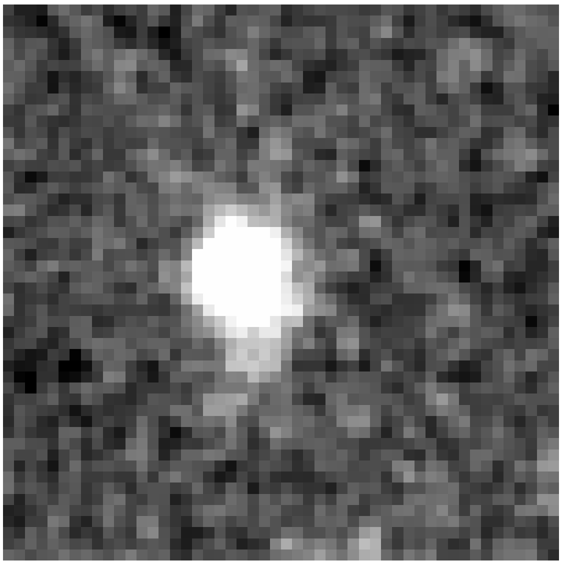

Figure C.12.: 530039676

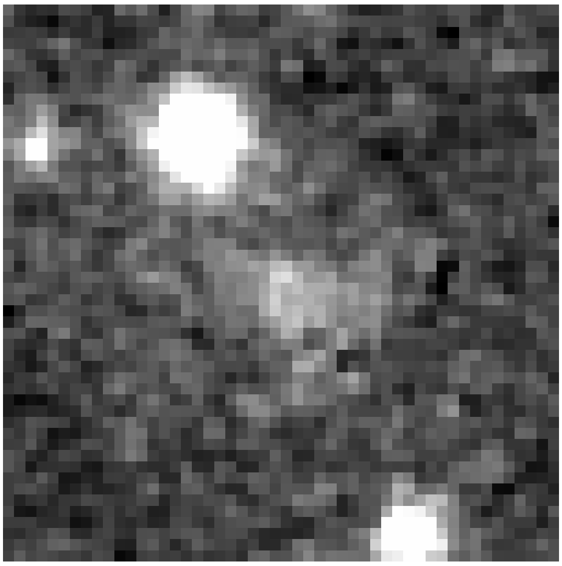

Figure C.13.: 530051196

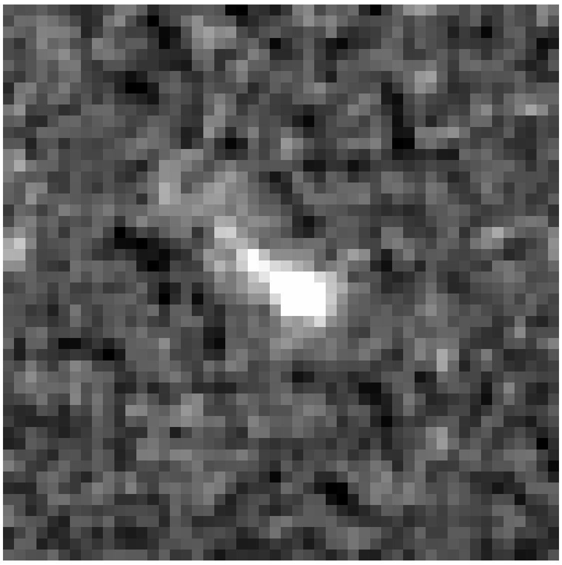

Figure C.14.: GOODSSB-25593749386